5-HT modulation of a medial septal circuit tunes social memory stability

https://doi.org/10.1038/s41586-021-03956-8

Received: 11 February 2021

Accepted: 25 August 2021

Published online: 6 October 2021

Check for updates

Xiaoting Wu[1], Wade Morishita[1], Kevin T. Beier[2], Boris D. Heifets[3] & Robert C. Malenka[1]✉

Social memory—the ability to recognize and remember familiar conspecifics—is critical for the survival of an animal in its social group[1,2]. The dorsal CA2 (dCA2)[3–5] and ventral CA1 (vCA1)[6] subregions of the hippocampus, and their projection targets[6,7], have important roles in social memory. However, the relevant extrahippocampal input regions remain poorly defined. Here we identify the medial septum (MS) as a dCA2 input region that is critical for social memory and reveal that modulation of the MS by serotonin (5-HT) bidirectionally controls social memory formation, thereby affecting memory stability. Novel social interactions increase activity in dCA2-projecting MS neurons and induce plasticity at glutamatergic synapses from MS neurons onto dCA2 pyramidal neurons. The activity of dCA2-projecting MS cells is enhanced by the neuromodulator 5-HT acting on 5-HT_{1B} receptors. Moreover, optogenetic manipulation of median raphe 5-HT terminals in the MS bidirectionally regulates social memory stability. This work expands our understanding of the neural mechanisms by which social interactions lead to social memory and provides evidence that 5-HT has a critical role in promoting not only prosocial behaviours[8,9], but also social memory, by influencing distinct target structures.

Since the discovery that the hippocampal dCA2 subregion is critical for social memory[3], research on this topic has focused on identifying additional storage sites in the hippocampus[5,6,10] and their respective output regions[5–7,11]. Little is known about the input regions to dCA2 or vCA1, which carry information about social encounters and are required for social memory formation. To identify hippocampal-projecting brain regions that are specifically involved in social memory, we exposed *TRAP2;Ai14* mice after injection with 4-hydroxytamoxifen (4-OHT) to a novel mouse, a novel object or an empty behavioural chamber to label neurons activated by these experiences, and examined brain regions that are not associated with object memory and project to dCA2 or vCA1 (Extended Data Fig. 1a). Increased numbers of tdTomato-positive cells were found in the MS and nucleus of the diagonal band (NDB) when comparing novel mouse to novel object and control conditions (Extended Data Fig. 1b). Interaction with a novel mouse also increased tdTomato-positive cells in dCA2 (Extended Data Fig. 1c, d). To determine whether, as previously suggested[3,12], neurons in different parts of the septum (lateral septum (LS), MS, NDB) form monosynaptic connections on hippocampal neurons, we used monosynaptic rabies tracing, which generated labelled cells in the MS and NDB, but not the LS (Extended Data Fig. 1e, f). Consistent with these and previous results[12], anterograde tracing revealed strong innervation of dorsal and ventral hippocampus (Extended Data Fig. 1g, h). Thus, MS and NDB neurons show increased activity during social encounters and project to dCA2 and vCA1.

Modulation of social memory by MS manipulations

The MS and NDB are implicated in hippocampal theta-rhythm[13] and arousal[14], but little is known about their potential roles in social behaviour. To determine whether the MS influences social memory, we expressed an inhibitory designer receptor exclusively activated by designer drugs (DREADD) fused to mCherry (hM4Di) or mCherry alone (mCh) in the MS of mice and administered the DREADD activator clozapine-*N*-oxide (CNO) or saline before a short-term social memory assay[6,7] (Fig. 1a, b). Two cohorts of control mice, expressing mCh and receiving CNO or expressing hM4Di and receiving saline, exhibited short-term (10-min interval) social memory as evidenced by their preference for the chamber containing a novel mouse compared to that containing a familiar mouse (Fig. 1c, Extended Data Fig. 2a). By contrast, hM4Di mice that received CNO exhibited no short-term memory of the familiar mouse (Fig. 1c, left). Calculating a discrimination score for each subject mouse, which enables more direct comparisons between treatments, confirmed the absence of social memory in mice in which MS neuronal activity was inhibited by hM4Di (Fig. 1c, right). Baseline sociability assessed during the initial, three-chamber sociability assay, as well as inanimate object memory, were not affected by hM4Di-mediated inhibition of the MS (Extended Data Fig. 2b, c).

We next addressed whether activation of MS neurons by the excitatory DREADD hM3Dq enhances social memory (Extended Data Fig. 2d). There was no effect of CNO administration in hM3Dq mice before the initial social interaction when social memory was assessed at 10 min (Extended Data Fig. 2e). However, this manipulation prolonged the duration of social memory to 2 h in the hM3Dq mice that received CNO but not in the two cohorts of control mice (Fig. 1d). Indeed, hM3Dq activation of MS neurons during the social interaction maintained social memory for 24 h (Extended Data Fig. 2e) but had no effects on baseline sociability (Extended Data Fig. 2f) or inanimate object memory (Extended Data Fig. 2g). To address whether the MS neurons that were activated during the initial social interaction are specifically necessary for social memory formation, we expressed Cre-dependent

[1]Nancy Pritzker Laboratory, Department of Psychiatry and Behavioral Sciences, Stanford University, Stanford, CA, USA. [2]Department of Physiology and Biophysics, University of California, Irvine, Irvine, CA, USA. [3]Department of Anesthesiology, Perioperative and Pain Medicine, Stanford University, Stanford, CA, USA. ✉e-mail: malenka@stanford.edu

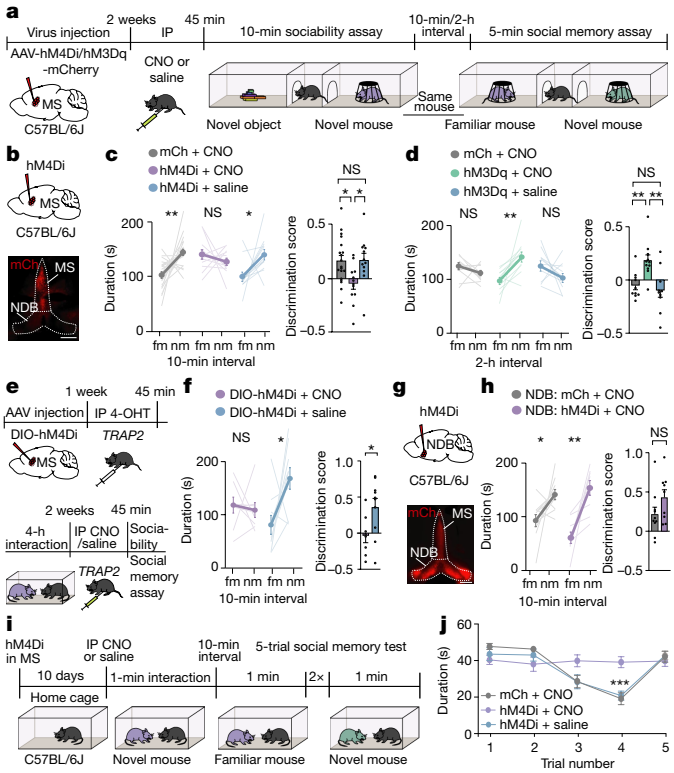

Fig. 1 | Chemogenetic manipulation of the MS bidirectionally regulates social memory. a, Experimental timeline of three-chamber tests. IP, intraperitoneal injection. **b**, Schematic and representative image of MS injection site. Scale bar, 500 µm. **c**, **d**, Left, duration that mice spent in the chamber with a familiar mouse (fm) or a novel mouse (nm). Right, discrimination scores (**c**: $F_{2,40} = 4.666$, $P = 0.0151$; mCh, $n = 19$; hM4Di, $n = 12$; **d**: $F_{2,28} = 8.585$, $P = 0.0012$; mCh, $n = 10$; hM3Dq, $n = 11$). **e**, Timeline of *TRAP2* experiment. **f**, Left, duration in chamber with a familiar mouse or a novel mouse. Right, discrimination scores ($t_7 = 2.594$, $P = 0.0357$; CNO, $n = 8$; saline, $n = 10$). **g**, Schematic and hM4Di expression in the NDB. Scale bar, 500 µm. **h**, Left, duration in chamber with a familiar mouse or a novel mouse. Right, discrimination scores ($t_{17} = 1.61$, $P = 0.1259$; mCh, $n = 10$; hM4Di, $n = 9$). **i**, Timeline of five-trial social memory test. **j**, Duration of direct interaction ($F_{27,108} = 2.478$, $P = 0.0005$; $n = 10$). Statistical tests: **c**, hM4Di + CNO, mCh + CNO duration; **d**, **f**, **h**, duration; **f**, discrimination scores: two-tailed paired Student's *t*-test. **c**, hM4Di + saline duration: two-tailed Wilcoxon signed rank test. **c**, **d**, Discrimination scores: one-way ANOVA with Tukey's post-hoc test. **h**, Discrimination scores: two-tailed unpaired Student's *t*-test. **j**, Two-way ANOVA with Tukey's post-hoc test. NS, not significant; $^*P < 0.05$, $^{**}P < 0.01$, $^{***}P < 0.001$. Error bars denote s.e.m.

hM4Di in the MS of *TRAP2* mice and exposed these mice to a novel mouse after administering 4-OHT (Extended Data Fig. 2h). Two weeks later, *TRAP2* mice that received saline before the social interaction exhibited normal social memory, which was blocked when the mice received CNO (Fig. 1e, f). Thus, the MS neurons that are activated by a novel social interaction are necessary for normal social memory formation.

To address whether the NDB is also required for social memory, we expressed hM4Di in the NDB but found that administration of CNO did not reduce social memory (Fig. 1g, h). As a final test of the role of the MS in social memory, we performed a five-trial social memory test[3]. As expected[3], by trials 3 and 4, the control mice spent less time interacting with the now familiar intruder mouse, but on trial 5 the time spent interacting with a novel mouse increased to baseline levels (Fig. 1i, j, Extended Data Fig. 2i). By contrast, the mice in which MS activity was inhibited (hM4Di + CNO) maintained equal interaction times for all five trials (Fig. 1j, Extended Data Fig. 2i).

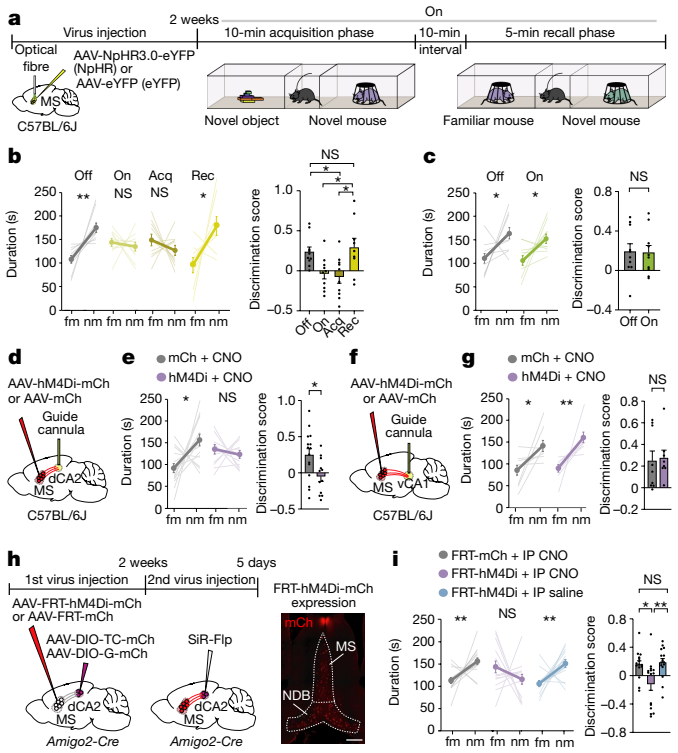

Fig. 2 | Inhibition of MS to dorsal CA2 projection disrupts social memory. a, Schematic of experiment. **b**, **c**, Left, duration that NpHR mice (**b**) or eYFP mice (**c**) spent in the chamber with a familiar mouse or a novel mouse. Right, discrimination scores (**b**: $F_{3,35} = 5.227$, $P = 0.0044$; $n = 10$; recall, $n = 9$; **c**: $t_9 = 0.1045$, $P = 0.919$; $n = 10$). Acq, acquisition phase; rec., recall phase. **d**, **f**, Schematic of CNO infusion into dCA2 (**d**) or vCA1 (**f**). **e**, **g**, Left, duration in chamber with a familiar mouse or a novel mouse. Right, discrimination scores (**e**: $t_{25} = 2.522$, $P = 0.0184$; mCh, $n = 15$; hM4Di, $n = 12$; **g**: $P = 0.4232$; mCh, $n = 9$; hM4Di, $n = 8$). **h**, Left, timeline of experiment. Right, hM4Di expression. Scale bar, 500 µm. **i**, Left, duration in chamber with a familiar mouse or a novel mouse. Right, discrimination scores ($P = 0.002$; $n = 15$). Statistical tests: **b**, **c**, **e**, duration; **c**, discrimination scores; **g**, **i**, mCh duration: two-tailed paired Student's *t*-test. **b**, Discrimination scores: one-way ANOVA with Tukey's post-hoc test. **e**, Discrimination scores: two-tailed unpaired Student's *t*-test. **g**, **i**, hM4Di duration: two-tailed Wilcoxon signed rank test. **g**, Discrimination scores: two-tailed Mann–Whitney test. **i**, Discrimination scores: Kruskal–Wallis with post-hoc Dunn's test. NS, not significant; $^*P < 0.05$, $^{**}P < 0.01$. Error bars denote s.e.m.

To address whether MS activity is necessary for memory acquisition and/or memory recall, we performed optogenetic manipulations by expressing the inhibitory halorhodopsin NpHR3.0 fused to eYFP (NpHR) or eYFP alone in the MS and providing light stimulation at various times during the social memory assay (Fig. 2a). Activation of NpHR throughout the procedure and during acquisition only disrupted social memory, whereas applying light during the recall phase had no effect (Fig. 2b). Social memory was also normal when NpHR mice were not exposed to light (Fig. 2b) and in eYFP mice that received light stimulation throughout the procedure (Fig. 2c). Similar to chemogenetic manipulations, optogenetic inhibition of the MS did not affect baseline sociability or inanimate object memory (Extended Data Fig. 3a–c).

Regulation of social memory by MS–dCA2 projections

Having established a critical role for the MS in social memory, we examined whether MS neuron projections to specific hippocampal subregions are required. We expressed hM4Di–mCh or mCh in the MS and implanted cannula above dCA2 or vCA1 to infuse CNO before the

sociability assay (Extended Data Fig. 3d). Infusion of CNO into dCA2 of hM4Di mice, but not into dCA2 of mCh mice, blocked social memory (Fig. 2d, e) and had no effects on baseline sociability and inanimate object memory (Extended Data Fig. 3e, f). By contrast, CNO infusion into vCA1 of hM4Di mice had no effect on social memory (Fig. 2f, g).

CNO may have spread to dCA1 and dCA3 and influenced MS projections to these regions. To manipulate the activity of MS neurons that specifically synapse on dCA2 pyramidal neurons, we applied an intersectional genetic strategy in *Amigo2-Cre* mice, a dCA2-specific Cre-driver line[3]. We injected adeno-associated viruses (AAVs) expressing Cre-dependent TVA and rabies glycoprotein into dCA2 and an AAV expressing Flp-dependent hM4Di–mCh or mCh into the MS (Fig. 2h). Two weeks later, we injected a rabies virus expressing Flp (ref. [15]) into dCA2 (Fig. 2h). Normal social memory was present in mCh mice administered CNO and in hM4Di mice administered saline but was absent in hM4Di mice administered CNO (Fig. 2i), with no differences between male and female mice (Extended Data Fig. 4a). DREADD-mediated inhibition of dCA2-projecting MS cells did not influence baseline sociability or inanimate object memory (Extended Data Fig. 4b, c). Because the MS is implicated in contextual memory[16] and aversion[17,18], which could influence social memory, we tested whether inhibition of this subset of MS cells influenced contextual fear conditioning or resulted in conditioned place preference or aversion. Fear conditioning was not affected by CNO administration in these hM4Di-expressing mice (Extended Data Fig. 4d) and had no effect in a conditioned place assay (Extended Data Fig. 4e).

To assess whether dCA2-projecting MS neurons send collaterals elsewhere, we used a marker to distinguish fibres of passage from axon terminals. We injected CAV-Flp into the dCA2 and Flp-dependent mGFP-synaptophysin-mRuby into the MS (Extended Data Fig. 4f). dCA2-projecting MS cells exhibited collaterals in the vCA1 and a smaller number in the supramammillary nucleus (Extended Data Fig. 4f). However, the MS collaterals innervating vCA1 are unlikely to be important for social memory as inhibiting the MS to vCA1 projection had no effect (Fig. 2g).

Plasticity at MS–dCA2 synapses

The MS contains a heterogeneous population of neurons[14,19]. To identify the MS cell types that synapse on dCA2 pyramidal neurons, we performed in situ hybridization to probe for cholinergic (*Chat*), glutamatergic (*Slc17a6*, gene name for VGLUT2) and GABAergic (γ-aminobutyric-acid-producing) (*Gad2*) markers in MS cells that were labelled by GFP through monosynaptic rabies tracing in dCA2 of *Amigo2-Cre* mice (Extended Data Fig. 5a, b). Quantification of *Gfp*-positive cells revealed that around 90% of dCA2-projecting MS cells are *Chat*-positive, around 30% are *Slc17a6*-positive and around 5% are *Gad2*-positive, with approximately 80% of *Slc17a6*-positive cells and 50% of *Gad2*-positive cells also being positive for *Chat* (Extended Data Fig. 5c, d). Immunohistochemistry confirmed that the majority of dCA2-projecting MS neurons express CHAT (around 60%), whereas a smaller proportion (around 40%) express calcium/calmodulin-dependent protein kinase II (CaMKII), a marker for glutamatergic neurons[20] (Extended Data Fig. 5e). To interrogate the functional role of cholinergic and glutamatergic inputs to dCA2 in social memory, we infused into dCA2 a mixture of muscarinic and nicotinic receptor antagonists or the NMDA receptor antagonist D-AP5 (Fig. 3a). Infusion of D-AP5 prevented social memory, which was not influenced by the blockade of cholinergic synaptic transmission or control infusion of saline (Fig. 3b). Baseline sociability was not influenced by any of these manipulations (Extended Data Fig. 5f, g) but inanimate object memory was prevented by infusion of the antagonists (Extended Data Fig. 5h), perhaps because of leakage into dCA1.

To investigate whether glutamatergic inputs from the MS elicit synaptic responses in dCA2 pyramidal neurons, we expressed

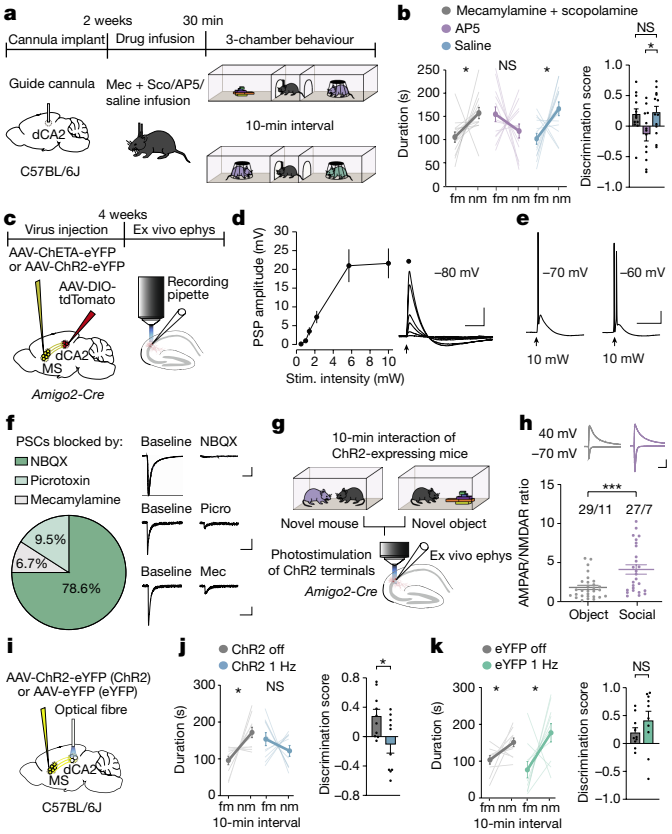

Fig. 3 | Glutamatergic inputs from the MS to dCA2 have a crucial role in social memory formation. a, Timeline for dCA2 drug infusions. AP5, D-AP5; Mec, mecamylamine; Sco, scopolamine. **b**, Left, duration that mice spent in the chamber with a familiar mouse or a novel mouse. Right, discrimination scores ($F_{2,36} = 4.017$, $P = 0.0266$; $n = 13$). **c**, Schematic of ex vivo electrophysiology (ephys). **d**, Current-clamp recordings from dCA2 neurons. Input–output graph of peak postsynaptic potential (PSP) ($n = 5/1$, cells/mice). Scale bars, 10 mV, 50 ms. **e**, Sample responses to stimulation at different membrane potentials. Scale bars, 20 mV, 50 ms. **f**, Left, percentage of cells in which the ChETA ($n = 20/9$) and ChR2 ($n = 22/6$) induced PSCs ($n = 42/15$) were more than 60% reduced by NBQX (10 μM), picrotoxin (50 μM) or mecamylamine (5 μM). Right, representative traces. Scale bars, 50 pA, 100 ms. **g**, Schematic of experiment. **h**, Bottom, AMPAR/NMDAR ratios in dCA2 neurons ($P = 0.0009$) of mice that interacted with a novel object ($n = 29/11$, cells/mice) or a novel mouse ($n = 27/7$). Top, representative traces. Scale bars, 100 pA, 100 ms. **i**, Schematic of in vivo optogenetic LTD induction. **j**, **k**, Left, duration in chamber with a familiar mouse or a novel mouse. Right, discrimination scores (**j**: $t_9 = 2.538$, $P = 0.0318$; $n = 10$; **k**: $t_9 = 1.155$, $P = 0.278$; $n = 10$). Statistical tests: **b**, duration; **j**, **k**: two-tailed paired Student's *t*-test. **b**, Discrimination scores: one-way ANOVA with Tukey's post-hoc test. **h**, Two-tailed Mann–Whitney test. NS, not significant; $^*P < 0.05$, $^{***}P < 0.001$. Error bars denote s.e.m.

channelrhodopsin-2 (ChR2) or a ChR2 variant (ChR2(E123T) accelerated; ChETA) in the MS of *Amigo2-Cre* mice and Cre-dependent tdTomato in dCA2 (Fig. 3c). Current-clamp recordings from visually identified, tdTomato$^+$ CA2 pyramidal neurons in ex vivo slices in response to optogenetic stimulation of MS inputs showed that excitatory postsynaptic potentials (EPSPs) were generated in all cells ($n = 5$). Increasing stimulation intensity increased EPSP amplitude (Fig. 3d) and generated action potentials (Fig. 3e). During voltage-clamp recordings, sequential application of the AMPAR antagonist NBQX, the GABA-A receptor antagonist picrotoxin and mecamylamine hydrochloride revealed that around 80% of neurons exhibited MS input-evoked postsynaptic currents (PSCs) that were substantially (more than 60%) reduced by NBQX, with less than 10% of neurons expressing PSCs that were reduced by picrotoxin or mecamylamine (Fig. 3f, Extended Data

Fig. 6a). These results suggest that the major functionally important inputs from MS to dCA2 pyramidal neurons are glutamatergic.

To investigate the role of synaptic strength changes at MS to dCA2 pyramidal cell synapses in social memory, we exposed *Amigo2-Cre* mice that express ChR2 in the MS and Cre-dependent tdTomato in dCA2 to a novel mouse or novel object and prepared slices immediately after the interaction (Fig. 3g). AMPAR/NMDAR ratios—a surrogate measure for synaptic strength[21]—in dCA2 neurons were increased after social interaction compared to object interaction (Fig. 3h), whereas paired-pulse ratios were unchanged (Extended Data Fig. 6b). If an increase in strength at MS to dCA2 pyramidal cell excitatory synapses during novel social interactions is required for social memory, reducing this increase should impair social memory. We first confirmed that low frequency (1 Hz for 5 min) optogenetic stimulation of MS inputs elicited a long-term depression (LTD) at synapses on dCA2 pyramidal neurons, which was not influenced by the application of muscarinic, nicotinic and GABA-A receptor antagonists (Extended Data Fig. 6c). Applying the same stimulation protocol (1 Hz for 5 min) in vivo to MS inputs in dCA2 (Fig. 3i, Extended Data Fig. 6d) immediately after memory acquisition to reduce the increase in synaptic strength generated by the novel social interaction prevented the expression of social memory (Fig. 3j). Similarly, applying low frequency stimulation (1 Hz for 10 min) in vivo before the initial social interaction also prevented social memory formation (Extended Data Fig. 7a). Notably, applying the same protocols in control mice expressing eYFP had no effect on social memory (Fig. 3k, Extended Data Fig. 7b) and no effects on baseline sociability or inanimate object memory in either ChR2-or eYFP-expressing mice (Extended Data Fig. 7c–h). These findings suggest that strengthening glutamatergic synapses from MS neurons onto dCA2 pyramidal neurons during a novel social encounter is required for normal social memory.

Social memory modulation by MS 5-HT$_{1B}$ receptors

How might MS neurons be influenced during a novel social interaction? MS neurons express receptors for oxytocin and 5-HT[22–24], neuromodulators that have roles in social behaviours[8,9]. To explore the potential role of oxytocin and 5-HT action in the MS in social memory, we infused oxytocin receptor (OXTR) or 5-HT receptor (5-HTR) antagonists into the MS before the social memory assay (Fig. 4a). Social memory was not influenced by infusion of saline or an OXTR antagonist (L-368,899 hydrochloride) but was prevented by infusion of the promiscuous 5-HTR antagonist, methiothepin maleate (Fig. 4b). Infusion of the broad 5-HT$_2$R antagonist methysergide or the 5-HT$_{1A}$R antagonist NAD-299 did not influence social memory, but infusion of the specific 5-HT$_{1B}$R antagonist NAS-181 impaired it (Fig. 4b). None of these manipulations had detectable effects on baseline sociability (Extended Data Fig. 8a). Because social memory was impaired by a 5-HT$_{1B}$R antagonist, we next tested whether a 5-HT$_{1B}$ agonist (CP93129) might prolong social memory in a manner similar to increasing MS neuron activity (Fig. 1d). Indeed, although social memory was again absent at 2 h after the initial social interaction in control mice, MS infusion of CP93129 before the social interaction resulted in social memory at 2 h (Fig. 4c).

Our findings predict that MS neuron activity increases during a novel social interaction in a 5-HT$_{1B}$R-dependent manner. To test this hypothesis, we expressed GCaMP6f in MS glutamatergic neurons and recorded MS neuron activity while the subject mouse had sequential interactions with a novel mouse; the same, now familiar mouse; a novel inanimate object; and, finally, another novel mouse (Fig. 4d, e). Activity in MS neurons increased robustly during interactions with a novel mouse whereas interactions with a familiar mouse or a novel inanimate object generated a smaller increase in MS neuron activity (Fig. 4f). Administration of NAS-181 reduced the increase in MS neuron activity during the novel mouse interaction (Fig. 4g), demonstrating the necessity of 5-HT$_{1B}$Rs. Similarly, the activity of MS cells that project to dCA2, captured by expressing CAV-Cre in dCA2 and Cre-dependent GCaMP6f in MS, was significantly higher during interaction with a novel mouse versus a familiar mouse or novel object and was also diminished after administration of NAS-181 (Fig. 4h–j).

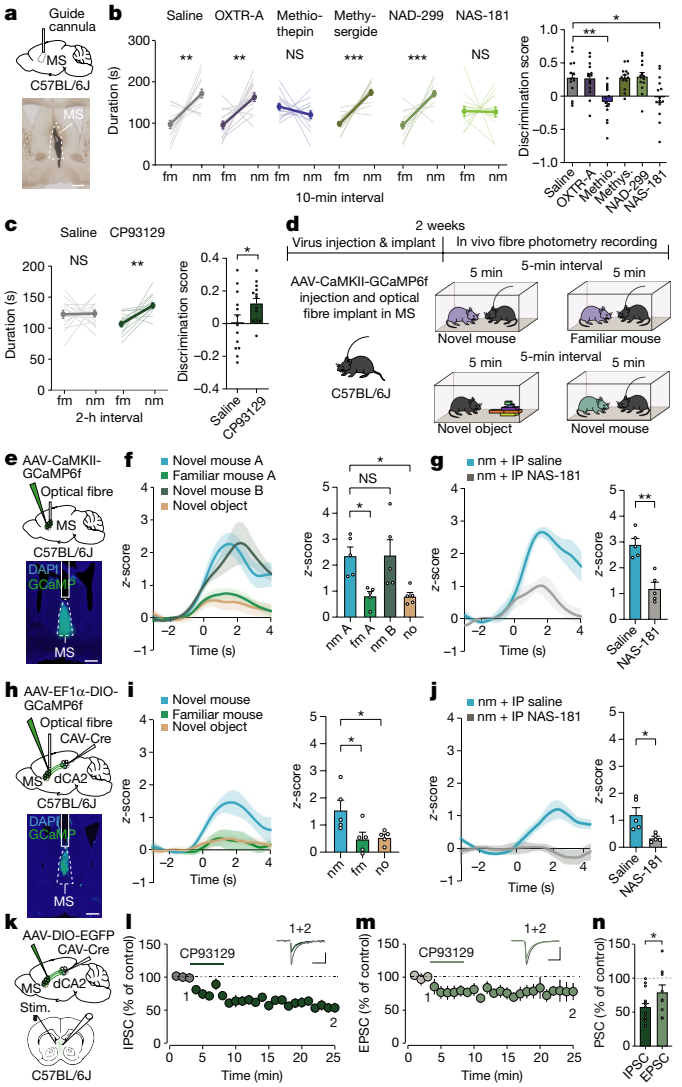

Fig. 4 | Bidirectional modulation of social memory by MS 5-HT$_{1B}$ receptors. **a**, Schematic and infusion site labelled with ink. Scale bar, 500 µm. **b**, **c**, Left, duration that mice spent in the chamber with a familiar mouse or a novel mouse. Right, discrimination scores (**b**: $F_{5,78} = 6.404$, $P < 0.0001$; $n = 14$. **c**: $t_{13} = 2.602$, $P = 0.0219$; $n = 14$). **d**, Schematic of fibre photometry experiment. **e**, **h**, Schematic and GCaMP6f expression (CaMKIIG–CaMP6f (**e**); Ef1α–DIO–GCaMP6f (**h**). Scale bars, 500 µm. **f**, **g**, **i**, **j**, Left, time courses of average GCaMP6f transient *z*-scores event-locked to direct interactions ('no', novel object). Right, quantification of average during interaction (**f**: $F_{3,16} = = 6.392$, $P = 0.0047$; $n = 5$; **g**: $t_4 = 5.103$, $P = 0.007$; $n = 5$; **i**: $F_{2,12} = 5.523$, $P = 0.0199$; $n = 5$; **j**: $t_4 = 3.752$, $P = 0.0199$; $n = 5$). **k**, Schematic of ex vivo electrophysiology set-up. **l**, Summary time course of IPSCs in response to CP93129 (5 µM) ($n = 15/7$ (cells/mice)). Top, representative traces recorded at indicated time points 1 and 2. Scale bars, 100 pA, 50 ms. **m**, Summary time course of EPSCs in response to CP93129 (5 µM) ($n = 9/4$). Top, representative traces. Scale bars, 100 pA, 10 ms. **n**, Average PSC (% of control) in the presence of CP93129 ($t_{22} = 1.854$, $P = 0.0386$; IPSC, $n = 9$; EPSC, $n = 15$). Statistical tests: **b**, duration; **c**, **g**, **j**: two-tailed paired Student's *t*-test. **b**, Discrimination score; **f**, **i**: one-way ANOVA with Tukey's post-hoc test. **n**, One-tailed unpaired Student's *t*-test. NS, not significant; $^*P < 0.05$, $^{**}P < 0.01$, $^{***}P < 0.001$. Error bars and shading denote s.e.m.

To address how 5-HT$_{1B}$Rs may contribute to increasing MS neuron activity during novel social interactions, we performed ex

vivo whole-cell recordings from visually identified dCA2-projecting MS neurons that were labelled by expression of CAV-Cre in dCA2 and Cre-dependent EGFP in MS (Fig. 4k). Application of the 5-HT_{1B}R agonist CP93129 (2.5 or 5 μM) generated an inward, depolarizing current in around 60–70% of dCA2-projecting MS neurons (Extended Data Fig. 8b–e). Because 5-HT_{1B}Rs are commonly presynaptic and inhibit neurotransmitter release[25], we hypothesized that activation of 5-HT_{1B}Rs depresses inhibitory synaptic transmission and increases MS neuron activity through 'disinhibition'. Consistent with this prediction, CP93129 decreased evoked inhibitory postsynaptic currents (IPSCs) by around 50% (Fig. 4l) and also depressed EPSCs to a smaller degree than IPSCs (Fig. 4m, n). These effects of CP93129 were not due to 'rundown' of synaptic currents, as EPSCs and IPSCs were stable for 45 min using identical recording conditions (Extended Data Fig. 8f–k). The depression of IPSCs is likely to be through a presynaptic action, as evidenced by a decrease in the frequency of spontaneous IPSCs and no effect on their amplitude (Extended Data Fig. 8l, m).

Modulation of social memory by MR 5-HT release

Our results suggest that social memory formation during a novel social interaction requires 5-HT release in the MS, which increases the activity of dCA2-projecting MS neurons through disinhibition. Consistent with the median raphe (MR) being a source of 5-HT in the MS[26], expressing Cre-dependent EGFP in the MR of *Sert-Cre* mice revealed 5-HTergic axon innervation in the MS (Extended Data Fig. 9a). Using TRIO (tracing the relationship between input and output) monosynaptic rabies virus tracing[27], we also observed labelling in the MR (Extended Data Fig. 9b), suggesting that there is direct synaptic input from the MR onto dCA2-projecting MS cells. To test the necessity of MR-mediated 5-HT release in the MS for social memory, we expressed Cre-dependent NpHR3.0–eYFP or eYFP alone in the MR of *Sert-Cre* mice and placed an optical fibre adjacent to the MS (Fig. 5a). Optogenetic inhibition of MR 5-HT inputs in the MS during the initial social interaction impaired social memory, which was normal in the control eYFP mice and when light was not applied to the NpHR mice (Fig. 5b, c). Baseline sociability and inanimate object memory were unaffected by these manipulations (Extended Data Fig. 9c–f).

To test whether enhancing 5-HT release in the MS influences the duration of social memory, we expressed ChR2–eYFP or eYFP in MR 5-HT neurons of *Sert-Cre* mice (Fig. 5d). Activation of 5-HT inputs in the MS during the initial novel social interaction generated social memory lasting 2 h, which was not present in the control conditions (Fig. 5e, f). Similar to previous results, these manipulations had no effects on baseline sociability (Extended Data Fig. 9g, h). To investigate whether our findings might have therapeutic implications, we generated mice that are haploinsufficient for neuroligins 1, 2 and 3 (*Nlgn123het* mice)[28]. Because *Nlgn3* knockout or mutation impairs social memory[29], but not sociability[30], we predicted that *Nlgn123het* mice would exhibit the same behavioural phenotype. Indeed, these mice exhibited normal baseline sociability (Extended Data Fig. 9i) but lacked social memory (Fig. 5h). Infusion of CP93129 into the MS rescued this social memory deficit (Fig. 5g, h) but had no effect on inanimate object memory (Fig. 5i) or sociability (Extended Data Fig. 9i).

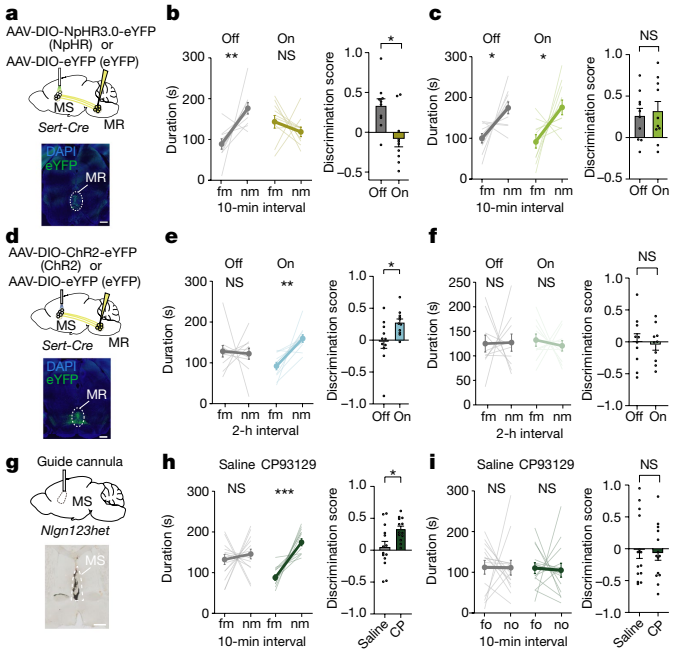

Fig. 5 | MR 5-HT release in the MS regulates social memory. a, **d**, Schematic and MR injection site (NpHR3.0–eYFP (**a**); ChR2–eYFP (**d**)). Scale bars, 500 μm. **b**, **c**, **e**, **f**, Left, duration that mice (NpHR mice (**b**) versus eYFP mice (**c**); ChR2 mice (**e**) versus eYFP mice (**f**)) spent in the chamber with a familiar mouse or a novel mouse. Right, discrimination scores (**b**: $t_9 = 2.27$, $P = 0.0493$; $n = 10$; **c**: $t_9 = 0.4444$, $P = 0.6672$; $n = 10$; **e**: $t_{10} = 2.471$, $P = 0.033$; $n = 11$; **f**: $t_9 = 0.2896$, $P = 0.7787$; $n = 10$). **g**, Schematic and MS infusion site filled with ink. Scale bar, 500 μm. **h**, Left, duration in chamber with a familiar mouse or a novel mouse. Right, discrimination scores ($t_{12} = 2.202$, $P = 0.048$; saline, $n = 14$; CP, $n = 13$). **i**, Left, duration in chamber with a familiar object (fo) or a novel object (no). Right, discrimination scores ($t_{13} = 0.3522$, $P = 0.7304$; $n = 14$). Two-tailed paired Student's *t*-test except for **e**, ChR2 off duration; **i**, saline duration: two-tailed Wilcoxon signed rank test. NS, not significant; $^*P < 0.05$, $^{**}P < 0.01$, $^{***}P < 0.001$. Error bars denote s.e.m.

Discussion

Previous work has established that the hippocampal dCA2 subregion has a specific role in social memory through its projections to vCA1[3,5], which in turn sends projections to the nucleus accumbens that are also required for social memory[6]. Here we show that increased activity in dCA2-projecting glutamatergic MS neurons during the initial social interaction is critical for social memory formation, probably because the strength of MS to dCA2 pyramidal neuron synapses increases. Furthermore, we show that dCA2-projecting MS neuron activity during a novel social interaction requires the MR-mediated release of 5-HT, which influences the stability of social memory through actions on 5-HT_{1B}Rs in the MS (Extended Data Fig. 10). Particularly notable were the findings that infusion of a 5-HT_{1B}R agonist into the MS prolongs the duration of social memory and rescues social memory deficits in an autism-associated mouse model. Given the role of neuroligins in synaptic function in CA1 pyramidal neurons[31], we surmise that the impairment of social memory in *Nlgn123het* mice may be due to deficient strength and/or plasticity at MS to dCA2 pyramidal neuron synapses and that administration of CP93129 into MS enhances activity in dCA2-projecting MS neurons in a manner that compensates for their synaptic communication deficit.

Our current model (Extended Data Fig. 10) suggests that 5-HT in the MS primarily works presynaptically to preferentially reduce the inhibition of dCA2-projecting MS neurons, perhaps through volume transmission[32,33] in a manner similar to the domain-overlap model proposed for dopamine[34]. However, we cannot rule out a role for 5-HT in acting directly on this population of neurons. Of note, none of our many manipulations of 5-HT action in the MS or MS neuron activity influenced basal sociability, suggesting that the appetitive value of a novel social interaction was not affected. Similar manipulations of 5-HT release in the nucleus accumbens have robust effects on sociability, also through 5-HT_{1B}Rs[8,9]. Furthermore, 5-HT action in other brain structures appears to be involved in aggression and perhaps impulsivity[35,36]. Thus, our results add to the growing evidence that global conclusions about the functions of neuromodulators such as 5-HT are not warranted.

Instead, the function of 5-HT or other neuromodulators needs to be considered in the context of the brain region in which they are acting.

5-HT neurons in the MR are heterogeneous and consist of a variety of distinct molecular subtypes[37,38], which may orchestrate different behaviours[39]. Therefore, it remains to be determined which specific subtypes of 5-HT MR neurons are critical for social memory and what role the release of other neurotransmitters from MR neurons, such as glutamate, might have[40]. It is also important to acknowledge that neuromodulators such as 5-HT do not act in isolation. The actions of both oxytocin[41,42] and dopamine[29] in structures other than the MS have been implicated in social memory, suggesting that a comprehensive understanding of how social memories form will require simultaneously examining the actions of multiple neuromodulators in a range of brain areas.

Online content

Any methods, additional references, Nature Research reporting summaries, source data, extended data, supplementary information, acknowledgements, peer review information; details of author contributions and competing interests; and statements of data and code availability are available at https://doi.org/10.1038/s41586-021-03956-8.

1. McGraw, L. A. & Young, L. J. The prairie vole: an emerging model organism for understanding the social brain. *Trends Neurosci.* **33**, 103–109 (2010).
2. Okuyama, T. Social memory engram in the hippocampus. *Neurosci. Res.* **129**, 17–23 (2018).
3. Hitti, F. L. & Siegelbaum, S. A. The hippocampal CA2 region is essential for social memory. *Nature* **508**, 88–92 (2014).
4. Leroy, F., Brann, D. H., Meira, T. & Siegelbaum, S. A. Input-timing-dependent plasticity in the hippocampal CA2 region and its potential role in social memory. *Neuron* **95**, 1089–1102 (2017).
5. Meira, T. et al. A hippocampal circuit linking dorsal CA2 to ventral CA1 critical for social memory dynamics. *Nat. Commun.* **9**, 4163 (2018).
6. Okuyama, T., Kitamura, T., Roy, D. S., Itohara, S. & Tonegawa, S. Ventral CA1 neurons store social memory. *Science* **353**, 1536–1541 (2016).
7. Phillips, M. L., Robinson, H. A. & Pozzo-Miller, L. Ventral hippocampal projections to the medial prefrontal cortex regulate social memory. *Elife* **8**, e44182 (2019).
8. Walsh, J. J. et al. 5-HT release in nucleus accumbens rescues social deficits in mouse autism model. *Nature* **560**, 589–594 (2018).
9. Heifets, B. D. et al. Distinct neural mechanisms for the prosocial and rewarding properties of MDMA. *Sci Transl Med* **11**, eaaw6435 (2019).
10. Chiang, M. C., Huang, A. J. Y., Wintzer, M. E., Ohshima, T. & McHugh, T. J. A role for CA3 in social recognition memory. *Behav. Brain Res.* **354**, 22–30 (2018).
11. Leroy, F. et al. A circuit from hippocampal CA2 to lateral septum disinhibits social aggression. *Nature* **564**, 213–218 (2018).
12. Chandler, J. P. & Crutcher, K. A. The septohippocampal projection in the rat: an electron microscopic horseradish peroxidase study. *Neuroscience* **10**, 685–696 (1983).
13. Buzsaki, G. Theta oscillations in the hippocampus. *Neuron* **33**, 325–340 (2002).
14. Kaifosh, P., Lovett-Barron, M., Turi, G. F., Reardon, T. R. & Losonczy, A. Septo-hippocampal GABAergic signaling across multiple modalities in awake mice. *Nat. Neurosci.* **16**, 1182–1184 (2013).
15. Ciabatti, E., Gonzalez-Rueda, A., Mariotti, L., Morgese, F. & Tripodi, M. Life-long genetic and functional access to neural circuits using self-inactivating rabies virus. *Cell* **170**, 382–392 (2017).
16. Sans-Dublanc, A. et al. Septal GABAergic inputs to CA1 govern contextual memory retrieval. *Sci. Adv.* **6**, aba5003 (2020).
17. Zhang, G. W. et al. Transforming sensory cues into aversive emotion via septal-habenular pathway. *Neuron* **99**, 1016–1028 (2018).
18. Zhang, G. W. et al. A non-canonical reticular-limbic central auditory pathway via medial septum contributes to fear conditioning. *Neuron* **97**, 406–417 (2018).
19. Papouin, T., Dunphy, J. M., Tolman, M., Dineley, K. T. & Haydon, P. G. Septal cholinergic neuromodulation tunes the astrocyte-dependent gating of hippocampal NMDA receptors to wakefulness. *Neuron* **94**, 840–854 (2017).
20. Meng, X. et al. Manipulations of MeCP2 in glutamatergic neurons highlight their contributions to Rett and other neurological disorders. *Elife* **5**, e14199 (2016).
21. Kauer, J. A. & Malenka, R. C. Synaptic plasticity and addiction. *Nat. Rev. Neurosci.* **8**, 844–858 (2007).
22. Sharma, K. et al. Sexually dimorphic oxytocin receptor-expressing neurons in the preoptic area of the mouse brain. *PLoS One* **14**, e0219784 (2019).
23. Cloez-Tayarani, I. et al. Autoradiographic characterization of [^{3}H]-5-HT-moduline binding sites in rodent brain and their relationship to 5-HT$_{1B}$ receptors. *Proc. Natl Acad. Sci. USA* **94**, 9899–9904 (1997).
24. Elvander-Tottie, E., Eriksson, T. M., Sandin, J. & Ogren, S. O. 5-HT$_{1A}$ and NMDA receptors interact in the rat medial septum and modulate hippocampal-dependent spatial learning. *Hippocampus* **19**, 1187–1198 (2009).
25. Sari, Y. Serotonin$_{1B}$ receptors: from protein to physiological function and behavior. *Neurosci. Biobehav. Rev.* **28**, 565–582 (2004).
26. Leranth, C. & Vertes, R. P. Median raphe serotonergic innervation of medial septum/diagonal band of broca (MSDB) parvalbumin-containing neurons: possible involvement of the MSDB in the desynchronization of the hippocampal EEG. *J. Comp. Neurol.* **410**, 586–598 (1999).
27. Schwarz, L. A. et al. Viral-genetic tracing of the input-output organization of a central noradrenaline circuit. *Nature* **524**, 88–92 (2015).
28. Jiang, M. et al. Conditional ablation of neuroligin-1 in CA1 pyramidal neurons blocks LTP by a cell-autonomous NMDA receptor-independent mechanism. *Mol. Psychiatry* **22**, 375–383 (2017).
29. Bariselli, S. et al. Role of VTA dopamine neurons and neuroligin 3 in sociability traits related to nonfamiliar conspecific interaction. *Nat. Commun.* **9**, 3173 (2018).
30. Etherton, M. et al. Autism-linked neuroligin-3 R451C mutation differentially alters hippocampal and cortical synaptic function. *Proc. Natl Acad. Sci. USA* **108**, 13764–13769 (2011).
31. Wu, X. et al. Neuroligin-1 signaling controls LTP and NMDA receptors by distinct molecular pathways. *Neuron* **102**, 621–635 (2019).
32. Bunin, M. A. & Wightman, R. M. Quantitative evaluation of 5-hydroxytryptamine (serotonin) neuronal release and uptake: an investigation of extrasynaptic transmission. *J. Neurosci.* **18**, 4854–4860 (1998).
33. Jennings, K. A. A comparison of the subsecond dynamics of neurotransmission of dopamine and serotonin. *ACS Chem. Neurosci.* **4**, 704–714 (2013).
34. Liu, C., Goel, P. & Kaeser, P. S. Spatial and temporal scales of dopamine transmission. *Nat. Rev. Neurosci.* **22**, 345–358 (2021).
35. Nelson, R. J. & Trainor, B. C. Neural mechanisms of aggression. *Nat. Rev. Neurosci.* **8**, 536–546 (2007).
36. Nautiyal, K. M. et al. Distinct circuits underlie the effects of 5-HT$_{1B}$ receptors on aggression and impulsivity. *Neuron* **86**, 813–826 (2015).
37. Okaty, B. W. et al. Multi-scale molecular deconstruction of the serotonin neuron system. *Neuron* **88**, 774–791 (2015).
38. Jensen, P. et al. Redefining the serotonergic system by genetic lineage. *Nat. Neurosci.* **11**, 417–419 (2008).
39. Baskin, B. M., Mai, J. J., Dymecki, S. M. & Kantak, K. M. Cocaine reward and memory after chemogenetic inhibition of distinct serotonin neuron subtypes in mice. *Psychopharmacology* **237**, 2633–2648 (2020).
40. Senft, R. A., Freret, M. E., Sturrock, N. & Dymecki, S. M. Neurochemically and hodologically distinct ascending VGLUT3 versus serotonin subsystems comprise the *r2-Pet1* median raphe. *J. Neurosci.* **41**, 2581–2600 (2021).
41. Ferguson, J. N. et al. Social amnesia in mice lacking the oxytocin gene. *Nat. Genet.* **25**, 284–288 (2000).
42. Raam, T., McAvoy, K. M., Besnard, A., Veenema, A. H. & Sahay, A. Hippocampal oxytocin receptors are necessary for discrimination of social stimuli. *Nat. Commun.* **8**, 2001 (2017).

Methods

Mice

Female and male C57BL/6J (JAX, 664), *TRAP2* (ref. [43]) (a gift from L. Luo), *TRAP2;Ai14* (a gift from L. Luo), B6.Cg-Tg(Amigo2-cre)1Sieg/J (*Amigo2-Cre*, JAX, 30215)[3], Tg(Slc6a4-cre)ET33Gsat (*Sert-Cre*, JAX, 3836639) and *Nlgn123het* mice were used as experimental subjects. A breeding strategy for the transgenic lines was used, in which strictly transgene-carrying male mice were crossed with wild-type female C57BL/6J mice sourced commercially to produce heterozygous offspring. *Nlgn123het* mice were generated by breeding *Nlgn123cKO*[28] (a gift from T. C. Südhof) male mice with B6.C-Tg(CMV-cre)1Cgn/J (JAX, 6054) females. Mice were weaned at 21 days old and housed with 2–5 mice per cage. Behavioural experiments were performed when mice were 7–14 weeks old. All mice were housed on a 12-h light–dark cycle with food and water ad libitum and behavioural experiments were conducted during the same circadian period (07:00–19:00). All procedures complied with the animal care standards set forth by the National Institutes of Health (NIH) and were approved by the Stanford University Administrative Panel on Laboratory Animal Care and Administrative Panel of Biosafety. No statistical methods were used to predetermine sample size, which was based on previous experience with the variance of the assays. All experiments were analysed without knowledge of the specific manipulation each mouse had undergone and performed without knowledge of the identity of the virus that had been injected or the transgene being expressed.

Stereotactic injections and cannula implantation

Mice, 4–7 weeks of age, were anaesthetized by intraperitoneal injection with a mixture of ketamine (75 mg per kg body weight) and dexmedetomidine (0.375 mg/kg body weight). Heads were fixed on a Kopf stereotaxic apparatus and holes were drilled bilaterally into the skull except for structures on the midline. For injections into specific brain regions the following bregma coordinates were used: dCA2, −1.6 mm anteroposterior (AP), ±1.6 mm mediolateral (ML), 1.7 mm dorsoventral (DV) from dura; MS, 0.65 mm AP, 0 mm ML, 4 mm DV; NDB, 1.25 mm AP, 0 mm ML, 5 mm DV; MR, −4.4 mm AP, 0 mm ML, 4.6 mm DV. Glass cannulas filled with virus solution were lowered to the specified depth from the dura and 0.5–1.5 µl of virus solution was injected using a microinjection pump (Harvard Apparatus) at a flow rate of 0.1–0.25 µl min^{-1}. After surgery, atipamezole (10 mg per kg body weight) was administered by intraperitoneal injection.

Adeno-associated viruses (AAVs) used for stereotactic injections were purchased from the Stanford Neuroscience Gene Vector and Virus Core and included: AAV_{DJ}-hSyn-EGFP, AAV_{DJ}-hSyn-hM4Di-mCherry, AAV_{DJ}-hSyn-DIO-hM4D(Gi)-mCherry, AAV_{DJ}-hSyn-fDIO-hM4D(Gi)-mCherry, AAV_{DJ}-hSyn-hM3D(Gq)-mCherry, AAV_{DJ}-hSyn-mCherry, AAV_8-EF1α-fDIO-mCherry, AAV_8-EF1α-NphR3.0-eYFP, AAV_{DJ}-EF1α-DIO-eYFP, AAV_{DJ}-EF1-ChETA-eYFP, AAV_{DJ}-hSyn-ChR2-eYFP, AAV_{DJ}-EF1α-DIO-tdTomato, AAV_{DJ}-CAMKII-GCaMP6f, AAV_{DJ}-EF1α-DIO-GCaMP6f, AAV_{DJ}-EF1α-DIO-NpHR3.0-eYFP, AAV_{DJ}-EF1α-DIO-ChR2-eYFP, AAV_{DJ}-EF1α-DIO-eYFP, AAV_{DJ}-CMV-DIO-EGFP and AAV-DJ-hSyn-FRT-mGFP-2A-Synaptophysin-mRuby[44]. AAV titres ranged from 1×10^{12} to 2×10^{13} gc ml^{-1}. CAV2-Cre[45] was purchased from E. Kremer (Institut de Génétique Moléculaire de Montpellier). For monosynaptic tracing, synapsin-driven lentiviral NLS-GFP-Cre, AAV-CAG-FLEx-TC, AAV-CAG-FLEx-G and rabies virus were obtained from Janelia Research Campus. The rabies virus expressing Flp (SIR-Flp)[15] was provided by K. Beier. Behavioural experiments involving manipulations of cell bodies were conducted 3–4 weeks after virus injections. The incubation time was 6–8 weeks for experiments involving manipulation of axon terminals.

For optogenetic behavioural experiments, optic fibres were implanted above the MS (coordinates: 0.65 AP, 0 ML, 3.5 DV) and dCA2 (−1.6 AP, ±1.6 ML, 1.2 DV). Optical implants were self-manufactured using 1.25-mm-diameter multimode ceramic ferrules (ThorLab), 200-µm fibre optic cable with numerical aperture (NA) 0.39 (ThorLabSA) and blue dye epoxy (Fibre Instrument Sales). For securing the optical implants to the skull, miniature screws (thread size 00–90 × 1/16, Antrin Miniature Specialties) and light-cured dental adhesive cement (Geristore A&B paste, DenMat) were applied. For drug infusions, a 26-gauge guide cannula (Plastics One) was first implanted bilaterally or unilaterally for midline structures into the brain region being studied. For dCA2 drug injection, the guide cannula was 0.9 mm in length from the cannula base and the infusers (essentially needles that fit into the guide cannula) for injections were 33-gauge and 2.4 mm in length. The cannulas for implantation above the vCA1 (coordinates: −3.16 AP, ±3.1 ML, 4 DV) were 2.8 mm in length and the infusers were 4.3 mm. The cannula implants for MS were 3.2 mm in length and the infusers were 4.7 mm. On the basis of visual histological analysis and blinded to the experimental results of the subject mice, a small percentage of the mice (around 5% of more than 300 mice) were excluded from behavioural analysis according to the following criteria: (1) off-target transgene expression (substantial somatic expression of fluorophore outside the region of interest by visual inspection); (2) weak transgene expression; or (3) inaccurate implant placement.

Intraperitoneal injection and cannula infusion of drugs

4-hydroxytamoxifen (4-OHT, Sigma H6278-50MG) was delivered via intraperitoneal (IP) injection at 50 mg kg^{-1} 45 min before behavioural experiments. Clozapine *N*-oxide (CNO, Tocris Biosciences 4936) was also given via IP injection at a concentration of 10 mg kg^{-1} 45 min before behavioural assays. For cannula microinjection experiments, 500 pg of CNO was infused in a total volume of 200 nl per side at a speed of 200 nl min^{-1} through an injector cannula using a microinfusion pump (Harvard Apparatus). The following drugs were also administered via microinjections at the same speed in a total volume of 400 nl–2 µl: AP-5 (Tocris Biosciences 0106, 2.4 µg), a mixture of mecamylamine hydrochloride (Tocris Biosciences 2843, 2 µg) and scopolamine hydrobromide (Tocris Biosciences 1414, 3 µg), L-368,899 hydrochloride (OXTR-A, Tocris Biosciences 2641, 0.25 µg), methiothepin mesylate salt (Millipore Sigma M149, 0.2 µg), methysergide maleate (Tocris Biosciences 1064, 0.5 µg), NAD-229 (Tocris Biosciences 3282, 3.5 µg), NAS-181 (Tocris Biosciences 1413, 2 µg) and CP93129 dihydrochloride (Tocris Biosciences 1032, 0.5 µg). Injection infusers were removed 2 min after completion of the fusion and mice were returned to their home cages for 30 min before behavioural assays. NAS-181 (10 mg kg^{-1}) was administered IP 30 min before fibre photometry experiments.

TRAP2 behavioural experiments

Mice were habituated for two days to IP injections (saline, 45 min prior) before placement in empty behavioural chambers (30 min, 23 cm length × 23 cm height × 25 cm width). On day three, female *TRAP2;Ai14* mice (4–6 weeks old) were injected with 4-OHT (50 mg kg^{-1}). Forty-five minutes later, mice were divided into three groups. Group 1 was placed in behavioural chambers with a novel female *TRAP2;Ai14* mouse. Group 2 was placed in the chambers with an inanimate object (for example, a Lego toy as shown in Fig. 1a) and group 3 was placed into an empty chamber. After 4 h, mice were returned to their home cages and 10 days later perfused with 4% paraformaldehyde (PFA) in PBS. The brains were placed into 4% PFA overnight and then cut on a vibratome into 60-µm slices. Images were acquired with an Olympus automated VS120 slide scanner (10× objective) and overlaid with images from Allen Brain Atlas for blinded manual counting of tdTomato-positive cells in specified brain regions.

Optogenetic stimulation

Mice were habituated for two days in the behavioural chambers with diodes (in off state) connected to their optic fibres. For photostimulation of NpHR3.0, optical implants were connected to a 532-nm laser diode (Shanghai Dream Lasers Technology) via a FC/PC adaptor and a fibre optic rotary joint (Doric Lenses). For photostimulation of ChR2, ferrules were connected to a 473-nm laser diode (OEM Laser Systems). A Master-8 pulse stimulator (A.M.P.I.) was used to control the laser, which was adjusted to around 8 mW for somatic stimulation

and around 15 mW for axon terminal stimulation using a digital power meter console (ThorLabs). To avoid tissue overheating when stimulating NpHR3.0, a light on–off cycle of 8 s on and 2 s off was applied. For ChR2 stimulation, 5-ms light pulses at 1 Hz were applied.

Three-chamber behavioural tests

Test mice were habituated to IP injections or to the fibre optic patch cord, depending on the experiment, as described above. They were also habituated to the three-chamber apparatus, which contained two empty upside-down metal grid pencil cups (10 cm in diameter) in the outer two chambers, for 5 min on two consecutive days. The three-chamber apparatus (72 cm length × 23 cm width × 25 cm height) was constructed of 0.635-cm-thick sheets of clear extruded acrylic for walls, and Komatex for floors (white) and barrier walls (black; TAP Plastics), with two outer chambers (28 cm length × 23 cm width) connected by a centre chamber (16 cm length × 23 cm width). The chambers were divided by translucent acrylic walls with 6.5-cm-diameter holes, 1 cm from the chamber floor. These dividers were removed during optogenetic experiments to allow subject mice to move freely with their patch cords attached. Mice placed under the cup were also habituated to the cup by spending 5 min under the cup on two consecutive days. On the test day, subject mice were placed in the middle chamber for 1 min, at which time the dividers were lifted, and the mice were allowed to explore the other two chambers freely for 10 min. One chamber contained an inanimate object, and the other chamber contained a novel mouse of the same sex. In the case of male mice, the mouse under the cup was a juvenile (3–5 weeks old). This session is referred to as a sociability test and was performed similarly to previously described methods[8]. The location of novel mice and objects was counterbalanced between sessions. After an interval of 10 min, 2 h or 24 h, subject mice were placed back into the middle chamber for 1 min at which time the barriers were removed, and the mice were allowed to freely explore for 5 min. During this social memory assay[6,7,46] one chamber contained a mouse under a cup from the previous session (familiar mouse) and the other chamber contained a novel mouse under a cup. Again, the location of novel mouse and familiar mouse was counterbalanced between sessions.

For analysis, a video tracking system (BIOBSERVE) was used to automatically track the location of the subject mouse during its free exploration. The sociability discrimination score was calculated as: [(time in novel mouse chamber − time in object chamber)/(time in novel mouse chamber + time in object chamber)]. The social memory discrimination score was calculated as: [(time in novel mouse chamber − time in familiar mouse chamber)/(time in novel mouse chamber + time in familiar mouse chamber)]. The object memory test was conducted in the same manner as the social memory test, with the difference that an object was placed into one chamber and the other chamber remained empty in the first session and the familiarized object was placed in one chamber and a novel object in another chamber in the second session. The same cohort of mice was used for social and object memory tests with the sequence of the two tests counterbalanced within the same cohort.

Female mice were used for the initial experiments illustrated in Figs. 1, 2a–g and Extended Data Figs. 1–3 to avoid potential confounds of aggressive behaviour between the subject mice and object mice under the cups. Beginning with the experiments illustrated in Fig. 2h and Extended Data Fig. 4, both male and female mice were used in all behavioural tasks and there was no sex difference between their discrimination scores in the sociability assays or social memory tests in any experimental condition. For all remaining experiments, both male and female subject mice were used in approximately equal numbers. Subject mice were excluded from the analysis (less than 2% of total), if they spent the entirety of the assay in only one chamber or if their velocity was 0 for more than 50% of the assay.

Five-trial social memory test

This test was performed as previously described[3,47]. Female C57BL/6J subject mice were individually housed for 7 days before the behavioural assay. On the day of testing, the mice were kept in their home cage and presented with a 10-week-old novel C57BL/6J female mouse for 4 successive 1-minute trials, interspersed by 10-min intervals. On the final trial, another novel mouse was presented. The trials were recorded, and the direct interaction time was scored manually and blinded to the experimental manipulation performed on the subject mouse.

Fear conditioning

Experiments were conducted in operant conditioning chambers (20 cm length × 24 cm width × 18 cm height, Med Associates) contained within sound-attenuating cubicles. The bottom of the chamber was composed of a metal grid, through which the foot shock was delivered. On day 1, mice received IP injections of CNO (10 mg kg^{-1}) 45 min before the experiment. Mice were individually placed into the fear conditioning chamber, which was illuminated by white light. After 2 min of free exploration, three foot shocks of 0.35 mA (lasting 2 s) were administered with an interval of 1 min. The subject mouse remained in the chamber for 1 min before being placed in a separate cage. After all mice from one cage underwent fear conditioning, all subject mice were returned to their home cage. After 24 h, mice were placed individually into the same chamber and per cent time freezing was analysed using video tracking software (BIOBSERVE).

Conditioned place preference

The experimental protocol was similar to that previously described[48]. On day 1, mice were tested for baseline preference by placing them in an unbiased chamber containing two interchangeable halves of flooring made of two textures. The 'grid' floor was composed of 13-cm acrylic rods (0.15-cm diameter) mounted 0.5 cm apart in acrylic rails (0.5 cm thick, surrounding all sides). The 'hole' floor was made out of perforated acrylic sheet with 8-mm round holes, 1 cm apart mounted on acrylic rails. Both floors (23 cm length × 14 cm width) were placed in the bottom of a black box (23 cm length × 23 cm width × 25 cm height). After 15 min of free exploration, mice were returned to their home cage. On day 2, mice were administered saline via IP injection 45 min before the conditioning. Each subject mouse explored the black box with either two hole or two grid flooring sections for 15 min. After 4 h, mice received an IP injection of CNO (15 mg kg^{-1}) and were placed 45 min later into the chamber containing two sections of the alternate flooring for 15 min. On day 3, mice were placed into the chamber containing both flooring types and time spent on either type of flooring was scored using video tracking software (BIOBSERVE).

Immunohistochemistry

Mice were perfused with 4% PFA or 10% formalin and brains were removed and post-fixed overnight at 4 °C. For procedures not involving immunohistochemistry (IHC) and in situ hybridization, 60–75-µm coronal sections were prepared on a vibratome. For IHC, brains were transferred to 30% sucrose for 48 h to cryo-preserve, mounted on the cryostat mounting disk with Tissue-Tek O.C.T. Compound (Sakura) on the tissue rack at −20 °C and sectioned on a cryostat into 40-µm slices. Free-floating sections were processed for immunohistochemistry. After three 10-min washes in PBS on a shaker, the tissue was incubated with blocking solution (5% normal goat serum or donkey serum and 0.3% Triton X-100 in PBS) for 45 min and then incubated in primary antibodies overnight at 4 °C on a shaker. The primary antibodies used were: rabbit polyclonal anti-CaMKII 1:200 (Thermo Fisher Scientific, PA5-38239), rabbit polyclonal anti-choline acetyltransferase (CHAT) 1:200 (Millipore Sigma, AB143), chicken anti-GFP 1:1,000 (Aves labs, GFP-1020). After three washes of 10 min in PBS, secondary antibodies were added and incubated for 3 h at room temperature on a shaker. The secondary antibodies used were: goat anti-rabbit Alexa Fluor 546 1:500 (Thermo Fisher Scientific, A11035), donkey anti-chicken Alexa Fluor 488 (Jackson Immuno Research Labs, 703545155). After three more washes the slices were mounted with Fluoromount-G mounting medium (Southern Biotech) onto microscopy slides for visualization at 10× using an Olympus automated VS120 slide scanner (UPLSAPO 10× objective, NA 0.4,

fluorescence light source: X-Cite 120LED light engine, filter cubes: DAPI, FITC, TRITC, Cy5, wavelength: 430–741 nm, XM10 camera, bit depth of images: 14 bit) or Nikon A1 confocal microscope (CFI Plan Apochromat Lambda 10× objective, NA 0.45, lasers: LU-N4/N4S 4-laser unit, 405 nm, 488 nm, 561 nm, 640 nm, filter cubes: 450/50, 525/50, 600/50, 685/70, 700/75, wavelength: 425–738 nm, detector: A1-DU4-2 4 Detector Unit: 4 Multi-Alkali PMTs, bit depth of images: 12 bit).

In situ hybridization

The experiment was carried out using the RNAscope Multiplex Fluorescent v2 kit and was performed according to the ACD Bio manual[49]. Brains were collected, fresh-frozen on dry ice and stored at −80 °C until sectioning on the cryostat. Fifteen-micrometre slices were prepared and collected directly on Superfrost plus microscopy slides. Following a 15-min fixation in prechilled 4% PFA, slices were rinsed twice in PBS and dehydrated gradually in higher concentrated ethanol in the order: 50%, 70%, two times 100% ethanol (5 min each). Slides were air-dried for 5 min and a barrier was drawn with a hydrophobic pen around the slices. Slides were then placed into a humidity control tray and incubated with around 5 drops of RNAscope hydrogen peroxide each for 10 min. After one wash with distilled water, slices were incubated with Protease IV for 30 min. After two washes in PBS, slices underwent a hybridization step in a probe mix for 2 h at 40 °C in a HyEZ Oven, at which time they were washed twice at room temperature in wash buffer (50× RNAscope Wash buffer diluted in distilled water). The following probes were used: RNAscope Probe-EGFP-C1 (400281), Mm-Gad2-C2 (415071-C2), Mm-Slc17a6-C3 (319171-C3), Mm-Chat-C4 (408731-C4). Probes were warmed up to 40 °C in a water bath for 10 min before use. 1 volume of C2, C3 and/or C4 were diluted in 50 volumes of C1. In the first amplification step, slides were incubated with around 6 drops of RNAscope Multiplex FL v2 Amp1 for 30 min at 40 °C in the HyEZ Oven and subsequently washed twice with wash buffer at room temperature This amplification step is repeated with RNAscope Multiplex FL v2 Amp2 and RNAscope Multiplex FL v2 Amp3, whereby the incubation time in Amp3 was only 15 min. For the development of the horse radish peroxidase (HRP) signal, slides were incubated with RNAscope Multiplex FL v2 HRP-C1 in the HyEZ Oven at 40 °C for 15 min and rinsed twice in wash buffer at room temperature. Afterwards, slides were incubated in 1:1,500 diluted Opal 520, 570, 620 or 690 (depending on the probe-dye combination) for 30 min at 40 °C and rinsed twice in wash buffer. This step was repeated with HRP-C2, HRP-C3 or HRP-C4 and different Opal dyes. In the final mounting step, Fluoromount-G mounting medium was dripped onto the slides and cover slips were placed over the slices. Slides were imaged on a Leica SP8 confocal (20× HC PL APO IMM CORR CS2 objective, NA 0.75, Argon laser, 65 mW, filter cubes: 458, 476, 488, 496, 514 nm, wavelength: 470–670 nm, detector: 5-channel confocal detection: 3 Hybrid-GaAsP detectors for increased light sensitivity, 2 standard fluorescent photomultiplier tubes (PMT), bit depth of images: 8 bit).

IHC and in situ quantification

All samples were imaged with the same settings to allow comparison between samples and background subtraction and thresholds were set uniformly for all images. Based on a pixel-intensity threshold, images were binarized and merged with DAPI in ImageJ[50]. A signal in a given channel that colocalized with DAPI was manually identified as a positive cell. Counting was conducted by visual scanning and with a manual cell counter.

Ex vivo electrophysiology

For recordings synaptic responses from dCA2 pyramidal neurons, 4–7 weeks after stereotactic injections of AAV_{DJ}-EF1-ChETA-eYFP or AAV_{DJ}-hSyn-Ch2-eYFP into the MS_{DJ} AAV_{DJ}-EF1α-DIO-tdTomato into dCA2, *Amigo2-Cre* mice were euthanized and brains were placed into sucrose cutting solution containing (in mM): 228 sucrose, 26 $NaHCO_3$, 11 glucose, 2.5 KCl, 1.2 NaH_2PO_4, 7 $MgCl_2$ and 0.5 $CaCl_2$ and sliced on a Leica vibratome. Coronal MS and hippocampal slices (200–250 µm) were transferred into artificial cerebrospinal fluid (ACSF) containing (in mM): 119 NaCl, 26 $NaHCO_3$, 11 glucose, 2.5 KCl, 1.2 NaH_2PO_4, 1.3 $MgCl_2$ and 2.5 $CaCl_2$ (osmolarity 289–295) for recovery at 32 °C for 30 min and then further 60 min of equilibration at room temperature. To evaluate the accuracy of injections, MS slices were placed in a recording chamber perfused with 28–30 °C ACSF equilibrated with 95% O_2 and 5% CO_2 and visualized with a 40× water-immersion objective on an upright fluorescent microscope (BX51WI; Olympus) equipped with infrared-differential interference contrast video microscopy and epifluorescence (Olympus). If MS neurons expressed eYFP, the hippocampal slices from that mouse were then placed in the recording chamber for optical stimulation. Whole-cell voltage-clamp recordings were made with pipettes (3–4 MΩ) filled with (in mM): 140 $CsMeSO_4$, 8 NaCl, 10 HEPES, 0.25 EGTA, 2 Mg_2ATP, 0.3 Na_3GTP, 0.1 spermine and 7 phosphocreatine (pH 7.29–7.36; osmolarity 290–295). Series and input resistance were continuously monitored with −4-mV, 70-ms pulse delivered through the recording pipette. Experiments were discarded if the series resistance varied by >15%. In some experiments CsMeSO4 was replaced with an equimolar concentration of KMeSO4 to perform current-clamp recordings or voltage-clamp recordings (for experiments in Extended Data Fig. 8b).

Whole-cell recordings were made from visually identified tdTomato-labelled pyramidal neurons in the CA2 while 473-nm 5-ms light pulses from the Opto Duet Laser system (IkeCool Corporation) were delivered to the whole slice via a 40× water-immersion objective on an Olympus microscope (BX51WI) at 0.1 Hz, thereby stimulating ChETA or ChR2 in MS axons and/or terminals. For voltage-clamp recordings, baseline PSCs were recorded at −70 mV for 5 min, at which time NBQX (10 µM) was added to the ACSF and PSCs recorded until their amplitudes were stable for 5 min. Then mecamylamine hydrochloride (5 µM) and in some cases scopolamine hydrobromide (5 µM) were added and PSCs assayed until stable for 5 min. The holding membrane potential was then adjusted to -50 mV and picrotoxin (50 uM) was applied to assess the contribution of GABA-A receptors to the PSCs. In 40% of cells, the order in which drugs were applied was shuffled with no detectable differences in their effects. For calculation of AMPAR/NMDAR ratios, the ACSF contained picrotoxin, mecamylamine hydrocholoride and scopolamine hydrobromide. The peak amplitude of an averaged AMPAR EPSC (n = 27–29 consecutive EPSCS measured at −70 mV) was divided by the amplitude of an averaged NMDAR EPSC (n = 27–29 measured at 50 ms after the onset of the EPSC at +40 mV). Paired-pulse ratios of averaged AMPAR EPSCs (n = 17–24) were calculated using a 50-ms interstimulus interval. To assess the strength of MS inputs to CA2 neurons (Fig. 3d) the peak amplitude was measured from an average of 10 consecutive EPSPs evoked at each light power. To elicit LTD at MS to dCA2 pyramidal neuron synapses in slices (Extended Data Fig. 6c), we applied 300 5-ms light pulses at 1 Hz. Summary graphs were generated by averaging individual EPSC measurements in 1-min bins and expressing each point as a percentage of the average of a 5-min baseline EPSC.

MS neurons projecting to dCA2 were labelled with EGFP by injection of CAV-Cre into dCA2 and Cre-dependent EGFP in the MS. Evoked EPSCs and IPSCs were recorded from EGFP-positive MS cells with a bipolar stimulating electrode (fabricated from platinum/iridium wire) placed near the recording pipette at 0.1 and 0.05 Hz, respectively. IPSCs and spontaneous IPSCs (sIPSCs) were recorded at −70 mV in the presence of NBQX (10 µM) and D-AP5 (50 µM). EPSCs were recorded at −70 mV in the presence of picrotoxin (50 µM). Summary graphs of the effects of CP93129 (Fig. 4l, m) and experiments controlling for pipette solution on evoked PSCs stability over time (Extended Data Fig. 8f, g) were generated by averaging the raw data in 1-min bins and expressing each point as a percentage of the averaged 3-min control. To increase IPSC signal to noise ratio, MS cells were chloride loaded with a pipette solution containing (in mM): 80 CsCl, 65 $CsMeSO_4$, 8 NaCl, 10 HEPES, 0.25 EGTA, 2 Mg_2ATP, 0.3 Na_3GTP, 0.1 spermine and 7 phosphocreatine

(pH 7.34; osmolarity 308). Cumulative probability graphs of sIPSCs were generated from a random sampling of 200 events before and in CP93129. The events for each experimental condition were arranged in ascending order and averaged. The resulting means and s.e.m. were plotted against their cumulative probability in the dataset. Intrinsic cell excitability was assessed with a series of incremental rectangular depolarizing current pulses (20 pA, 500 ms) injected into MS cells while recording in current-clamp. Drug-induced changes in the number of action potentials were determined by the number of action potentials evoked in the presence of no applied holding current. In cells in which CP93129 increased excitability, a graph was constructed plotting action potential number versus injected current. Peak currents induced by CP93129 (2 or 5 μM) were defined as those that could be clearly distinguished (>10 pA) as an agonist-induced inward or outward event from baseline. Recordings were made using a MultiClamp 700B amplifier (Molecular Devices), digitized at 10 kHz with the Digidata 1320A or 1440A data acquisition system (Molecular Devices), and analysed using Axograph or custom software written for Igor Pro (Wavemetrics). sIPSCs were analysed with MiniAnalysis (Synaptosoft).

Fibre photometry

Fibre photometry was performed as previously described[9]. AAV_{DJ}-CaMKII-GCaMP6f or AAV_{DJ}-EF1α-DIO-GCaMP6f was injected into the MS and CAV-Cre was injected into the dCA2. Fibre optic implants (Doric) were inserted and secured above the MS (0.65 AP, 0 ML, 3.5 DV). After 2–3 weeks, mice were habituated to the behavioural set-up for 10 min and tested one day later with simultaneous video and fibre photometry acquisition. On the test day, mice were placed in one chamber of the three-chamber apparatus, which was barricaded to create a small single chamber. Direct interaction with a novel mouse, a familiar mouse and a novel object was monitored for 5 min with an interval of 5 min. The presentation sequence of mouse and object was counterbalanced between subject mice. Fibre photometry data were acquired using the Synapse software, which controls an RZ5P lock-in amplifier (Tucker-Davis Technologies). During acquisition GCaMP6f was excited by frequency-modulated 473- and 405-nm light-emitting diodes (Doric), to stimulate Ca^{2+}-dependent and isosbestic emission, respectively. All optical signals were band-pass-filtered with a fluorescence mini cube (Doric), emission was measured with a femtowatt photoreceiver (2151; Newport), and signal was digitized at 6 kHz. MATLAB (MathWorks) was used for signal processing, including correction of motion artifact and fluorescent bleaching. Signals were debleached by fitting with a mono- or bi-exponential decay function, and the resulting fluorescence trace was *z*-scored. Videos were manually analysed and the time of every physical contact after approach from a distance of more than 2 cm between subject mouse and an object or mouse was determined. An average of 7-s non-overlapping epochs of fluorescence was used to construct peristimulus time histograms. The time of contact is defined as time = 0, positioned in between 3 s before and 4 s after contact time. For each subject mouse, 2–7 contacts occurred per session and these were averaged to obtain the *z*-score graph for that mouse. Peak *z*-scored fluorescence was the maximal *z*-score between 0 and 4 s.

Statistical methods and reproducibility

The experimenter was blinded to the virus injection the animals had received. All analyses were performed with the experimenter blinded to the manipulation that the subject mouse had received. All data were tested for normality of sample distributions and when violated, non-parametric statistical tests were used. One-way ANOVA with Tukey's multiple comparison post-hoc test was performed to assess significance for multiple group comparisons and two-way ANOVA with Tukey's or Sidak's multiple comparison post-hoc test for multiple group comparisons across multiple time points. Whenever ANOVA is performed, *P* values in the figure legends indicate the ANOVA results of the whole group, whereas the asterisks between individual samples are the results of the multiple comparison post-hoc tests. Two-tailed paired Student's *t*-tests were used for within-group comparison of two treatments and the unpaired test was used for comparison between two groups. When normal distributions were not assumed, the Wilcoxon signed rank tests was performed for within group comparisons of two treatments, Mann-Whitney for between group comparison, and Kruskal-Wallis with post-hoc Dunn's test for multiple comparisons. NS, not significant. $^{*}P < 0.05$, $^{**}P < 0.01$, $^{***}P < 0.001$. In all figures, data are shown as mean ± s.e.m.

Fig. 1b: 1 out of 12 mice; Fig. 1g: 1 out of 9 mice; Fig. 2h: 1 out of 15 mice; Fig. 4a: 1 out of 14 mice; Fig. 4e, h: 1 out of 5 mice; Fig. 5a: 1 out of 10 mice; Fig. 5d: 1 out of 11 mice; Fig. 5g: 1 out of 13 mice.

Reporting summary

Further information on research design is available in the Nature Research Reporting Summary linked to this paper.

Data availability

The datasets generated and analysed during this study are included in this published article and its supplementary information files. Any additional data generated during and/or analysed during this study are available from the corresponding author upon reasonable request. Source data are provided with this paper.

Code availability

Code used for data processing and analysis is available from the corresponding author upon reasonable request. The MATLAB code used for analyses of fibre photometry data is provided as a supplementary file.

43. Allen, W. E. et al. Thirst-associated preoptic neurons encode an aversive motivational drive. *Science* **357**, 1149–1155 (2017).
44. Beier, K. T. et al. Circuit architecture of VTA dopamine neurons revealed by systematic input-output mapping. *Cell* **162**, 622–634 (2015).
45. Kremer, E. J., Boutin, S., Chillon, M. & Danos, O. Canine adenovirus vectors: an alternative for adenovirus-mediated gene transfer. *J. Virol.* **74**, 505–512 (2000).
46. Hung, L. W. et al. Gating of social reward by oxytocin in the ventral tegmental area. *Science* **357**, 1406–1411 (2017).
47. Ferguson, J. N., Young, L. J. & Insel, T. R. The neuroendocrine basis of social recognition. *Front. Neuroendocrinol.* **23**, 200–224 (2002).
48. Cunningham, C. L., Gremel, C. M. & Groblewski, P. A. Drug-induced conditioned place preference and aversion in mice. *Nat. Protoc.* **1**, 1662–1670 (2006).
49. Wang, F. et al. RNAscope: a novel in situ RNA analysis platform for formalin-fixed, paraffin-embedded tissues. *J. Mol. Diagn.* **14**, 22–29 (2012).
50. Cardozo Pinto, D. F. et al. Characterization of transgenic mouse models targeting neuromodulatory systems reveals organizational principles of the dorsal raphe. *Nat. Commun.* **10**, 4633 (2019).

Acknowledgements This work was supported by philanthropic funds donated to the Nancy Pritzker Laboratory at Stanford University. X.W. was supported by a NIH K99 Career Development Award (MH122697). K.T.B. was supported by NIH grant DP2 AG067666. B.D.H. was supported by a NIH K08 Career Development Award (MH110610). We thank B. S. Bentzley for providing assistance with the fear conditioning experiments; P. A. Neumann and S. R. Golf for providing mouse breeding pairs; and members of the Malenka laboratory for discussions. Extended Data Fig. 10 schematic by Sci Stories, LLC.

Author contributions X.W. conceived the study and performed the majority of experiments. X.W. and R.C.M. designed the experiments, interpreted the results and wrote the paper, which was edited by all authors. W.M. and X.W. performed the ex vivo electrophysiology experiments. K.T.B. prepared and provided Flp-expressing rabies virus. B.D.H. contributed to the design and analysis of fibre photometry experiments, including hardware configuration and creating analysis scripts in MATLAB.

Competing interests All protocols used during this study are freely available for non-profit use from the corresponding author upon reasonable request. R.C.M. is on the scientific advisory boards of MapLight Therapeutics and MindMed.

Additional information
Supplementary information The online version contains supplementary material available at https://doi.org/10.1038/s41586-021-03956-8.

Correspondence and requests for materials should be addressed to Robert C. Malenka.

Peer review information *Nature* thanks Susan Dymecki and the other, anonymous, reviewer(s) for their contribution to the peer review of this work.

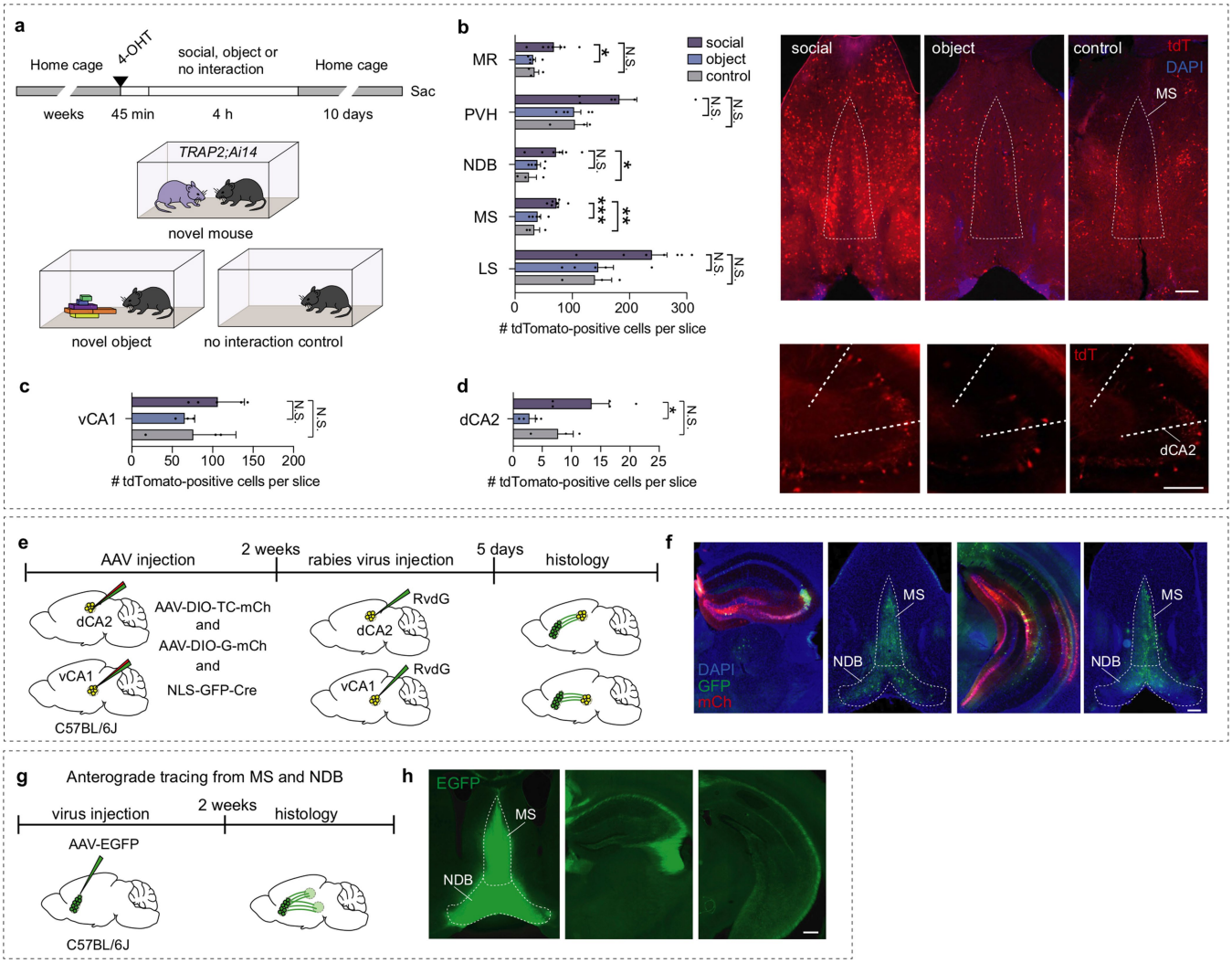

Extended Data Fig. 1 | MS cells show increased cFOS after a social experience. a, Schematic of experimental timeline, 4-OHT was administered via intraperitoneal injection. **b**, Quantification of tdTomato-positive cells in the median raphe (MR: $F_{2,12} = 4.681$, $P = 0.0314$), paraventricular nucleus of the hypothalamus (PVH: $F_{2,11} = 3.446$, $P = 0.0689$), nucleus of the diagonal band (NDB: $F_{2,12} = 4.423$, $P = 0.0364$), medial septum (MS: $F_{2,12} = 13.31$, $P = 0.0009$), lateral septum (LS: $F_{2,12} = 4.14$, $P = 0.0429$) in the social ($n = 7$), object ($n = 5$) and control ($n = 3$) conditions. Representative images of MS expressing tdTomato. Scale bar, 200 µm (right). **c**, Quantification of tdTomato-positive cells in the ventral CA1 (vCA1: $F_{2,8} = 1.478$, $P = 0.2842$) in social ($n = 5$), object ($n = 3$) and control ($n = 3$) conditions. **d**, Quantification of tdTomato-positive cells in the dorsal CA2 (dCA2: $F_{2,9} = 5.367$, $P = 0.0292$) in social ($n = 5$), object ($n = 4$) and control ($n = 3$) conditions. Representative images of dCA2 expressing tdTomato. Scale bar, 200 µm (right). **e**, Schematic of monosynaptic tracing experiment. **f**, Representative images of injection site in the dorsal hippocampus and presynaptic labelling in the MS (left), injection site in the ventral hippocampus and presynaptic labelling in the MS (right). Scale bar, 200 µm, $n = 3$. **g**, Schematic of anterograde tracing experiment. **h**, Representative images of injection site in the MS (left) and axon terminals in the dorsal and ventral hippocampus (right). Statistical tests: **b**–**d**, One-way ANOVA with Tukey's post-hoc test, N.S. = not significant, $^*P < 0.05$, $^{**}P < 0.01$, $^{***}P < 0.001$ (left). Scale bar, 200 µm, $n = 3$. Error bars denote s.e.m.

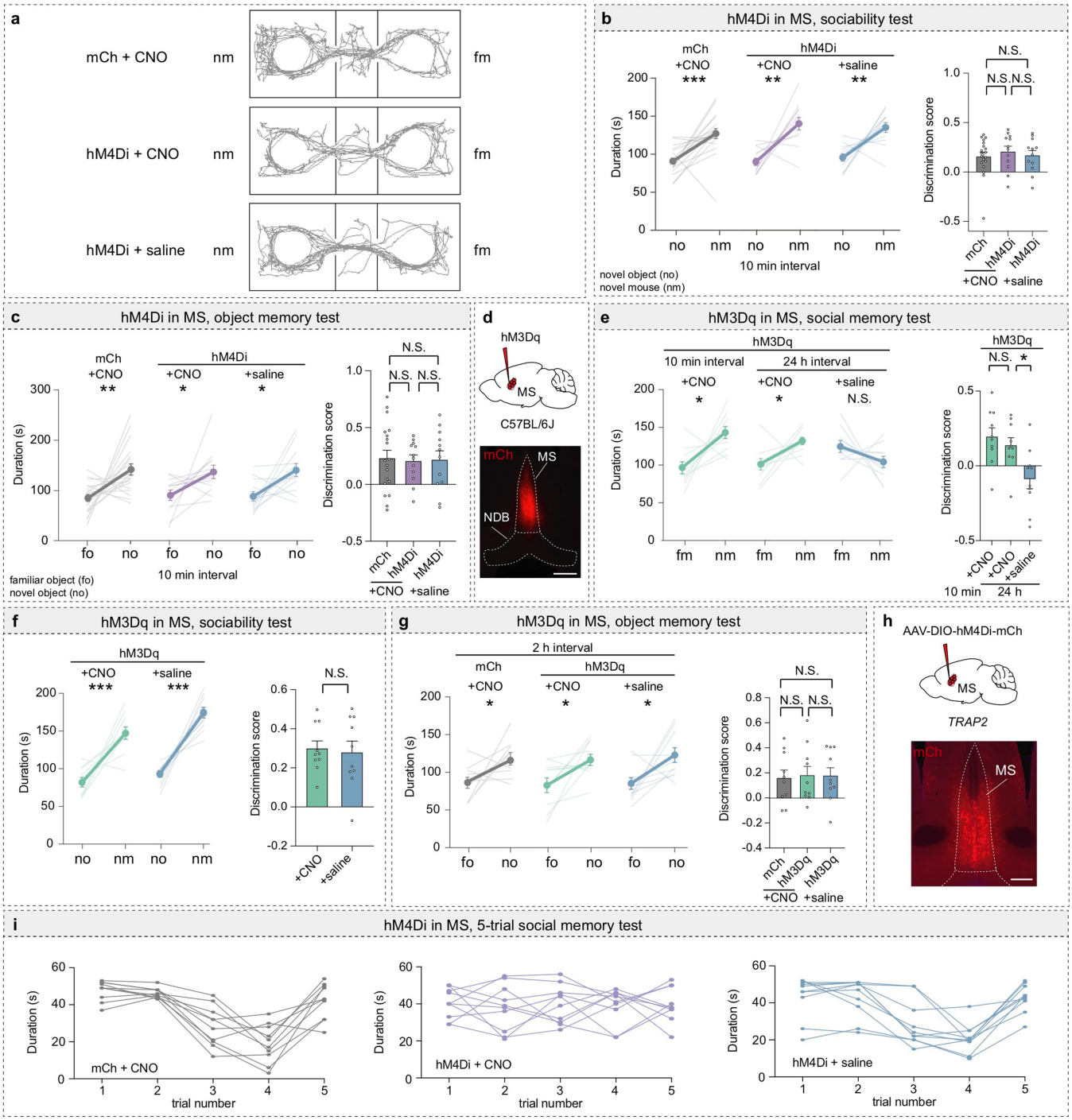

Extended Data Fig. 2 | Chemogenetic manipulation of the MS does not affect sociability and object memory. a, Representative traces of subjects during three-chamber social memory test. **b**, Duration in chamber with novel object (no) or novel mouse (nm) (left) and discrimination scores (right) ($F_{2,40} = 0.2875$, $P = 0.7517$; mCh: $n = 19$, hM4Di: $n = 12$). **c**, Duration in chamber with familiar object (fo) or no (left) and discrimination scores (right) ($F_{2,40} = 0.04521$, $P = 0.9558$; mCh: $n = 19$, hM4Di: $n = 12$). **d**, Schematic and representative image of MS injection site showing hM3Dq expression. $n = 10$. Scale bar, 500 µm. **e**, Duration in chamber with fm or nm (left) and discrimination scores (right) ($F_{2,27} = 6.689$, $P = 0.0044$, $n = 10$). **f**, Duration with no or nm (left) and discrimination scores (right) ($t_9 = 0.2358$, $P = 0.8189$; $n = 10$). **g**, Duration with familiar object (fo) or no (left) and discrimination scores (right) ($F_{2,27} = 0.3243$, $P = 0.9681$; $n = 10$). **h**, Schematic and representative image of hM4Di expression in the MS. $n = 8$. Scale bar, 500 µm. **i**, Individual subjects from Fig. 1j. Statistical tests: **b**, **c**, **e**, **f**, **g**, duration: two-tailed paired Student's *t*-test. **b**, **c**, **e**, **g**, Discrimination scores: one-way ANOVA with Tukey's post-hoc test. **f**, Discrimination scores: two-tailed paired Student's *t*-test. N.S. = not significant, $^{*}P < 0.05$, $^{**}P < 0.01$, $^{***}P < 0.001$. Error bars denote s.e.m.

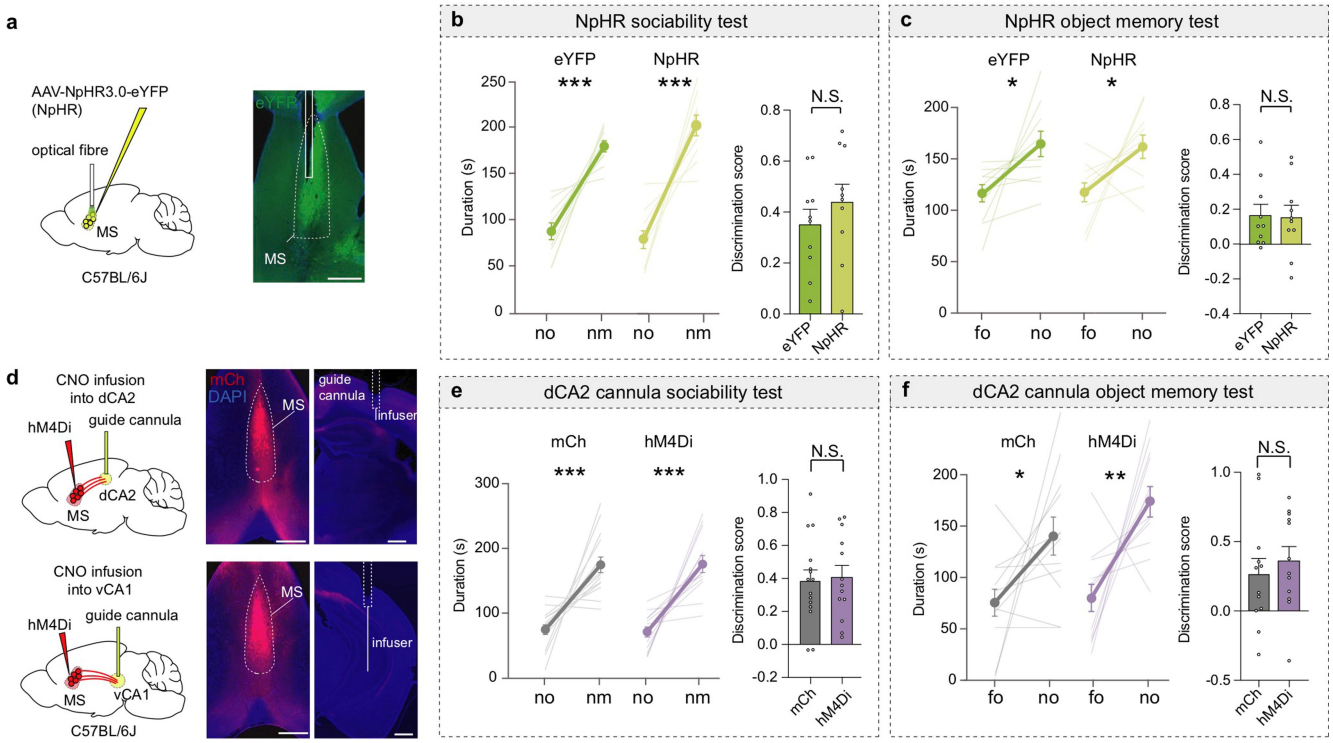

Extended Data Fig. 3 | Optogenetic MS cell body and chemogenetic terminal inhibition do not affect sociability and object memory. **a**, Schematic of experimental set-up (left) and representative image of MS injection site showing NpHR expression (right). $n = 10$. Scale bar, 500 µm. **b**, Duration in chamber with no or nm (left) and discrimination scores (right) ($t_{18} = 0.9531$, $P = 0.3532$; $n = 10$). **c**, Duration in chamber with fo or no (left) and discrimination scores (right) ($t_{18} = 0.1348$, $P = 0.8943$; $n = 10$). **d**, Schematic of experimental set-up (left) and representative images of MS injection sites showing hM4Di expression and cannula implant sites (right). $n = 13$. Scale bar, 500 µm. **e**, Duration in chamber with no or nm (left) and discrimination scores (right) ($t_{26} = 0.2453$, $P = 0.8081$; mCh: $n = 15$, hM4Di: $n = 13$). **f**, Duration in chamber with fo or no (left) and discrimination scores (right) ($t_{22} = 0.6383$, $P = 0.5298$; $n = 12$). All data were assessed by two-tailed unpaired Student's t-test. N.S. = not significant, $^*P < 0.05$, $^{***}P < 0.001$. Error bars denote s.e.m.

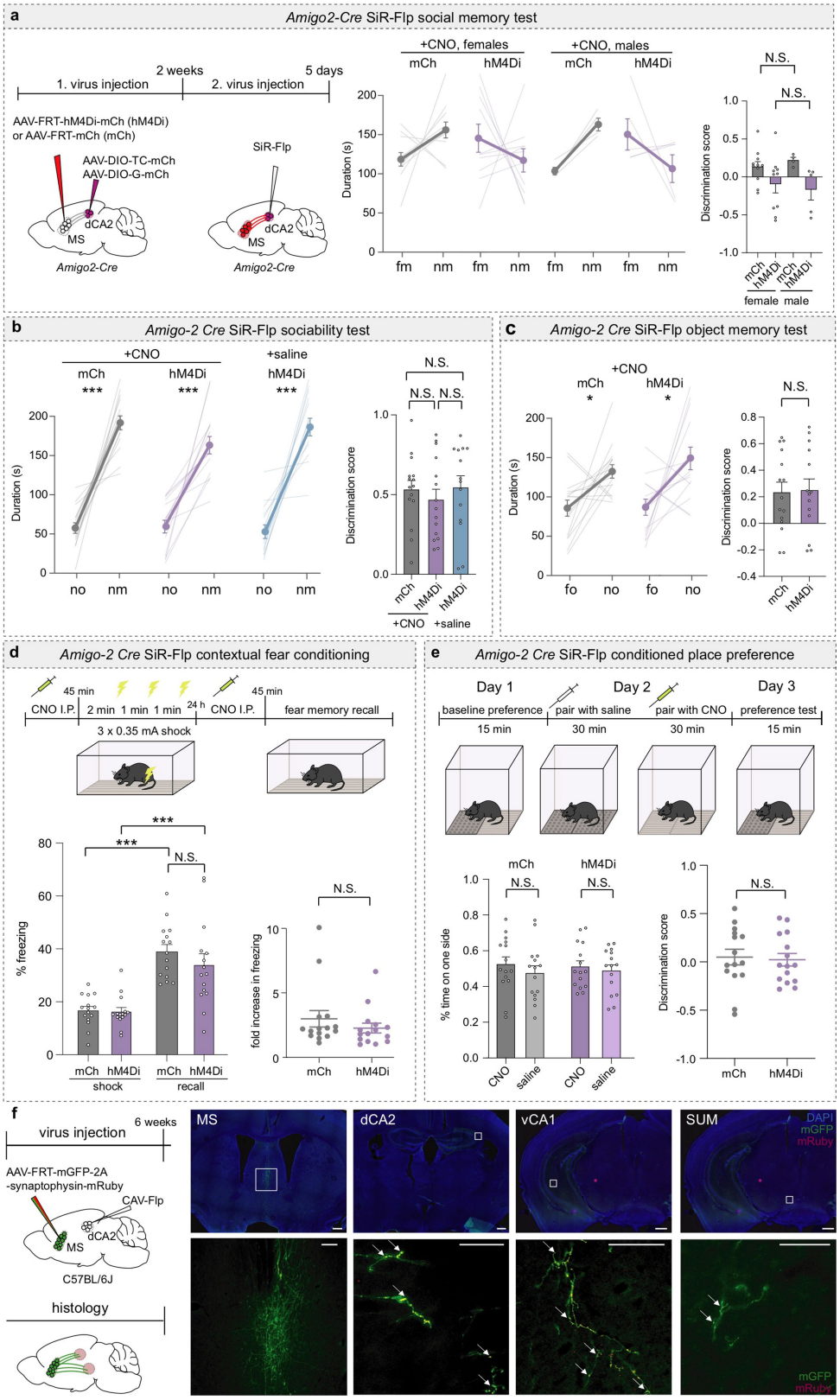

Extended Data Fig. 4 | See next page for caption.

Extended Data Fig. 4 | Inhibition of dCA2-projecting MS neurons has no effect on sociability, object memory, contextual fear memory and conditioned place preference. a, Schematic of experimental set-up (left). Duration in chamber with fm or nm (middle) and discrimination scores (right) (hM4Di: $P = 0.5135$; female mCh: $n = 11$, hM4Di: $n = 10$, male mCh: $n = 4$, hM4Di: $n = 5$). **b**, Duration in chamber with no or nm (left) and discrimination scores (right) ($F_{2,42} = 0.4013$, $P = 0.6721$; $n = 15$, hM4Di+saline: $n = 14$). **c**, Duration with fo or no (left) and discrimination scores (right) ($t_{27} = 0.1384$, $P = 0.891$; mCh: $n = 15$, hM4Di: $n = 14$). **d**, Schematic of experimental set-up (top) and quantification of the percent freezing during shock and recall (bottom left) and fold increase in freezing time (bottom right) ($P = 0.2671$; $n = 15$). **e**, Schematic of experimental set-up (top), quantification of the percent time spent on each surface after CNO and saline pairing (bottom left) and discrimination scores (bottom right) ($t_{28} = 0.2619$, $P = 0.7953$; $n = 15$). **f**, Schematic of virus injection, left. Representative images of MS injection site as well as the labelled axon in the dCA2, ventral CA1 (vCA1) and supramammillary nucleus (SUM), right ($n = 3$, scale bars = 500 µm above and 200 µm below; arrows point to mRuby puncta. Statistical tests: **a**, two-tailed Mann-Whitney test. **b**, **c**, Duration: two-tailed paired Student's *t*-test. **b**, Discrimination score: one-way ANOVA with Tukey's post-hoc test **c**, **e**, Discrimination scores: two-tailed unpaired Student's *t*-test. **d**, % freezing: Kruskal–Wallis with post-hoc Dunn's test, fold-increase in freezing: two-tailed Mann-Whitney test. **e**, % time on one side: one-way ANOVA with Tukey's post-hoc test. N.S. = = not significant. $^{*}P < 0.05$, $^{**}P < 0.01$, $^{***}P < 0.001$. Error bars denote s.e.m.

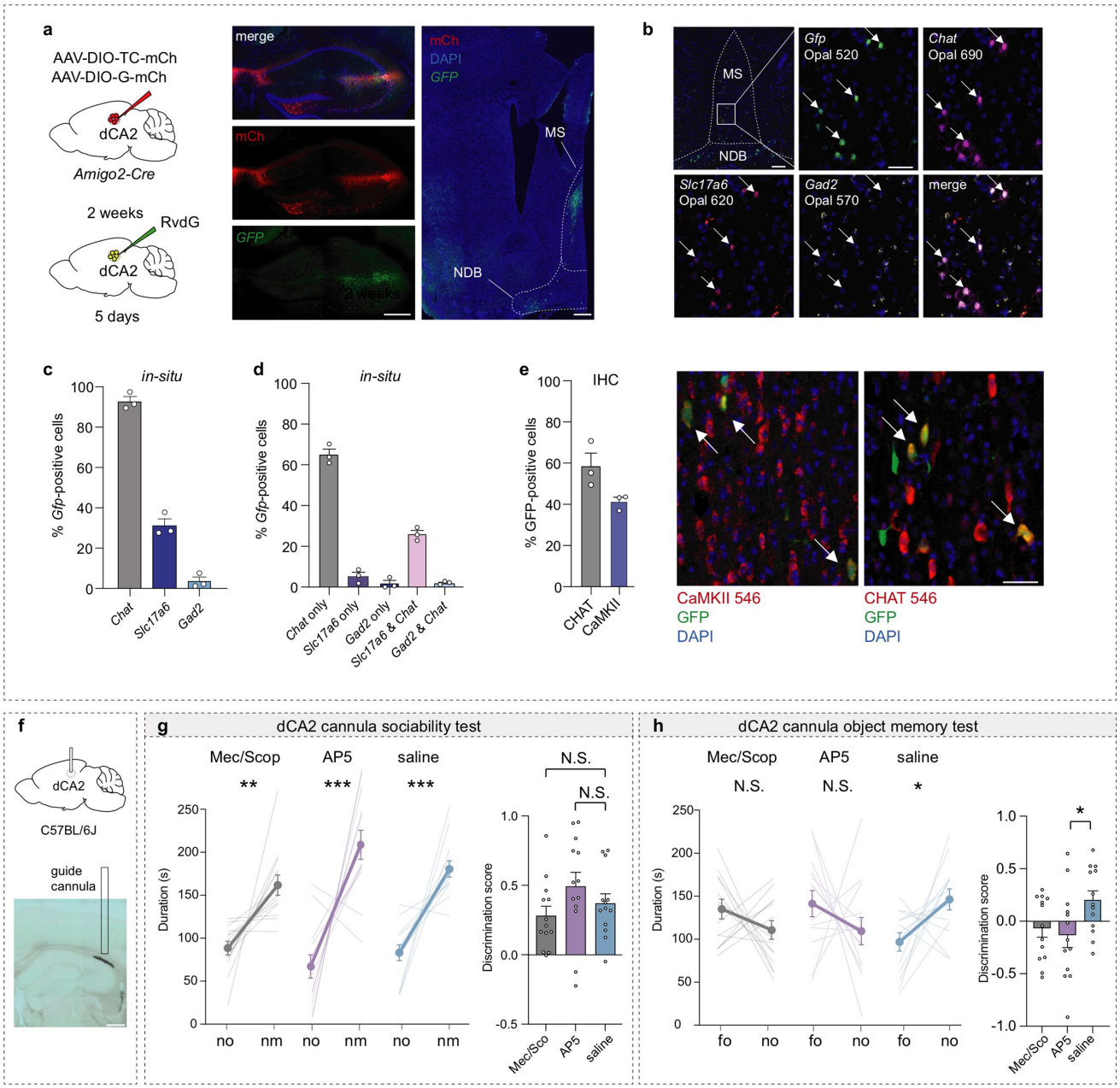

Extended Data Fig. 5 | dCA2-projecting MS cells are primarily cholinergic and glutamatergic. a, Schematic of monosynaptic rabies tracing set-up in *Amigo2-Cre* mice (left) and representative images of injection site in the dCA2 as well as *Gfp*-positive cells in the MS (right). Scale bar, 200 µm, $n = 3$. **b**, Representative images of *in-situ* hybridization. Scale bar, 200 µm (upper left panel), 40 µm. **c**, Quantification of *in-situ* hybridization, $n = 3$ subjects. **d**, Quantification of same *in-situ* hybridization data for percent of *Gfp*-positive cells colocalizing with *Chat* only, *Slc17a6* only, *Gad2* only or double-positive for *Slc17a6* and *Chat*, *Gad2* and *Chat* (right), $n = 3$ subjects. **e**, Quantification of colocalization with GFP-positive cells via immunohistochemistry (IHC) using either CHAT or CaMKII antibodies (left) and representative images (right, scale bar, 40 µm, $n = 3$). **f**, Schematic of experimental set-up and representative image of dCA2 infusion site filled with ink. **g**, Duration in chamber with no or nm (left) and discrimination scores (right) ($F_{2,36} = 1.702$, $P = 0.1967$; $n = 13$). **h**, Duration in chamber with fo or no (left) and discrimination scores (right) ($F_{2,36} = 3.259$, $P = 0.05$; $n = 13$). Statistical tests: **g**, **h**, duration: two-tailed paired Student's *t*-test; discrimination scores: one-way ANOVA with Tukey's post-hoc test. N.S. = not significant, $^{*}P < 0.05$, $^{**}P < 0.01$, $^{***}P < 0.001$. Error bars denote s.e.m.

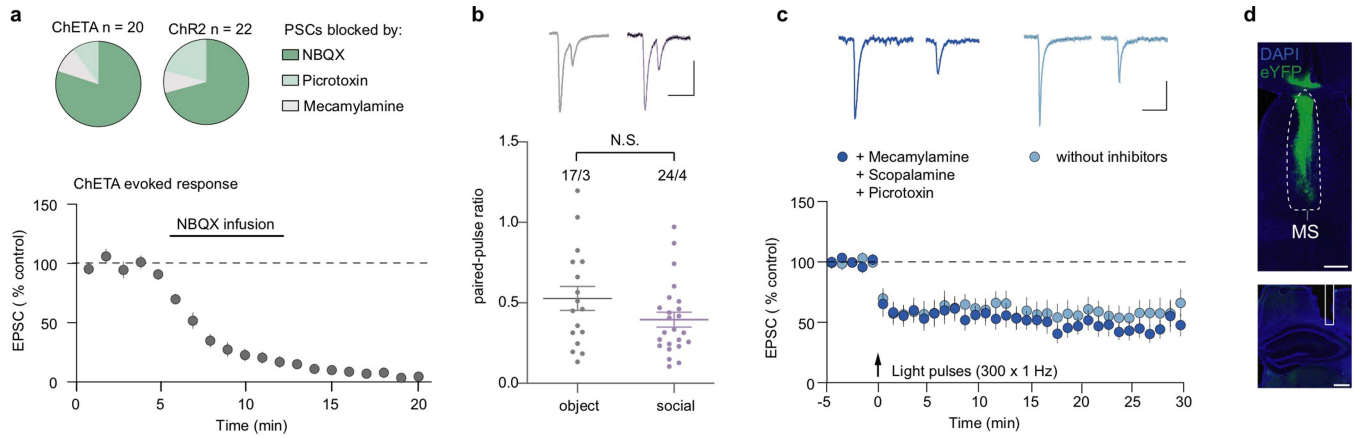

Extended Data Fig. 6 | MS synapses onto dCA2 pyramidal neurons are primarily glutamatergic and can express long-term depression ex vivo. **a**, Top, pie charts of percentage of cells, in which the ChETA (n = 20/9) and ChR2 (n = 22/6) induced PSCs were >60% reduced by NBQX (10 µM), picrotoxin (50 µM) or Mecamylamine (5 µM). Below, summary time course of ChETA-evoked PSCs from tdTomato-positive dCA2 pyramidal neurons, which were completely blocked (>90%) by bath-application of NBQX (n = 13). **b**, Representative traces of PSCs evoked by paired-pulse MS input activation in slices prepared from *Amigo2-Cre* mice exposed to a novel object or novel mouse (social). Scale bars, 50 pA, 100 ms. Quantification of paired-pulse ratios for mice (below) interacting with a novel object (n = 17/3, cells/mice) or novel mouse (n = 24/4) (t_{39} = 1.589, P = 0.1201), two-tailed unpaired Student's t-test. N.S. = not significant. **c**, Representative EPSCs from tdTomato-positive dCA2 pyramidal neurons before and after LTD induction protocol. Scale bars, 25 pA, 100 ms. Summary time-course of EPSCs with and without listed receptor antagonists in bath. With inhibitors: n = 8/4, without inhibitors: n = 6/3. **d**, Representative image of MS ChR2 injection site (above) and optical fibre implant site in the dCA2 (below). n = 10. Scale bars, 500 µm. Error bars denote s.e.m.

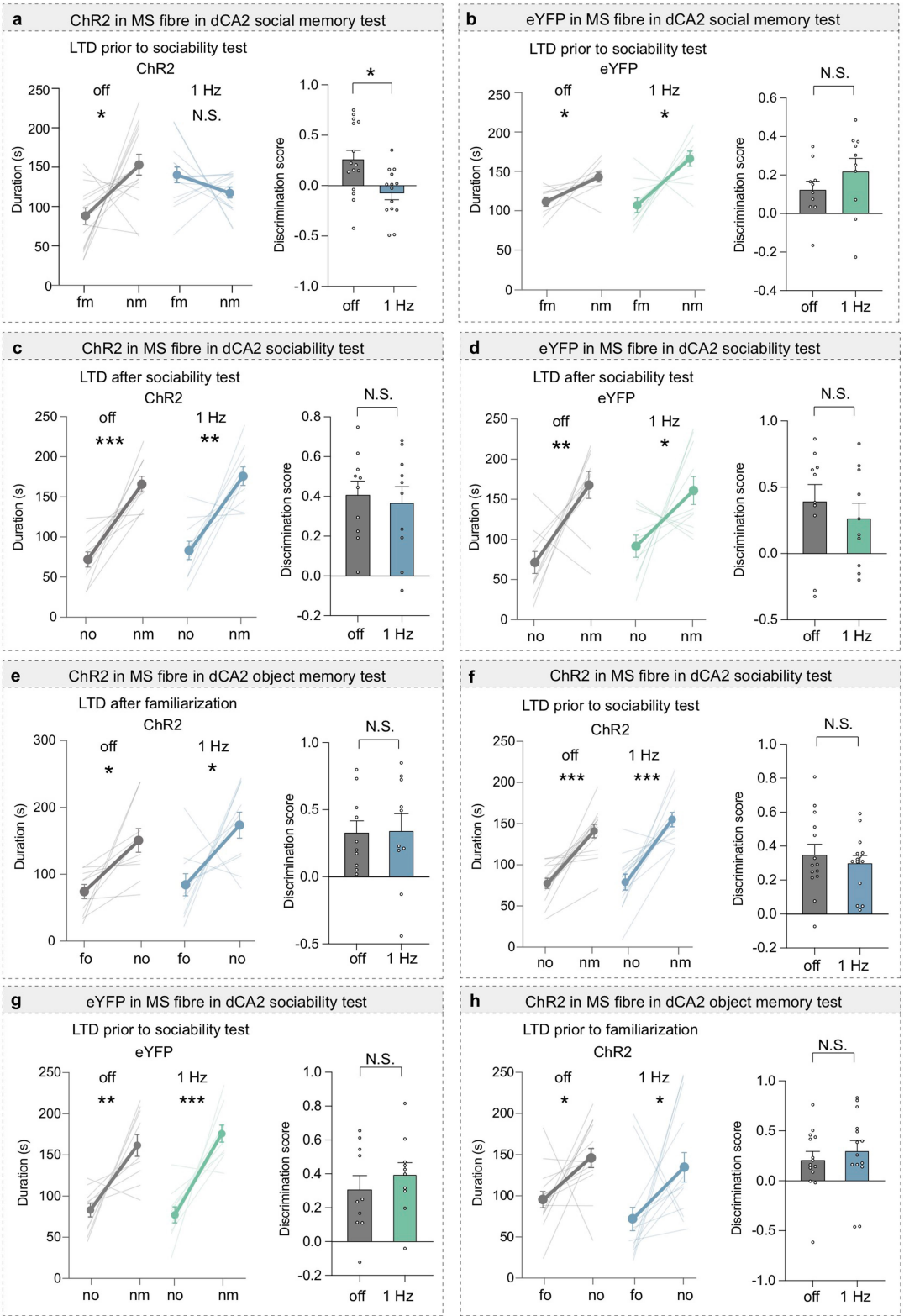

Extended Data Fig. 7 | Effects of in vivo optogenetic low frequency stimulation to induce LTD at MS to dCA2 synapses on sociability, social memory and object memory. a, **b**, Duration in chambers with fm or nm (left) and discrimination scores (right), LTD stimulation (1 Hz for 10 min) was performed prior to sociability test, (**a**: $t_{13} = 2.898$, $P = 0.0125$; off: $n = 15$, 1 Hz: $n = 14$. **b**: $t_9 = 0.9806$, $P = 0.3524$; $n = 10$). **c**, **d**, Duration in chamber with no or nm, left and discrimination scores (right) in ChR2 and eYFP mice, LTD stimulation (1 Hz for 5 min) was performed after sociability test (**c**: $t_9 = 0.3201$, $P = 0.7563$; $n = 10$, **d**: $t_9 = 0.6328$, $P = 0.5426$; $n = 10$). **e**, Duration with fo or no (left) and discrimination scores (right) ($t_9 = 0.09968$, $P = 0.9228$; $n = 10$) in ChR2 mice. **f**, **g**, Duration in chamber with no or nm, left and discrimination scores (right) in ChR2 and eYFP mice (**f**: $t_{13} = 0.7717$, $P = 0.4540$; $n = 14$, **g**: $t_9 = 1.208$, $P = 0.2577$; $n = 10$). **h**, Duration with fo or no (left) and discrimination scores (right) ($t_{13} = 0.6186$, $P = 0.5469$; $n = 14$) in ChR2 mice. Two-tailed paired Student's t-test was performed on all data. N.S. = not significant, $^*P < 0.05$, $^{**}P < 0.01$, $^{***}P < 0.001$. Error bars denote s.e.m.

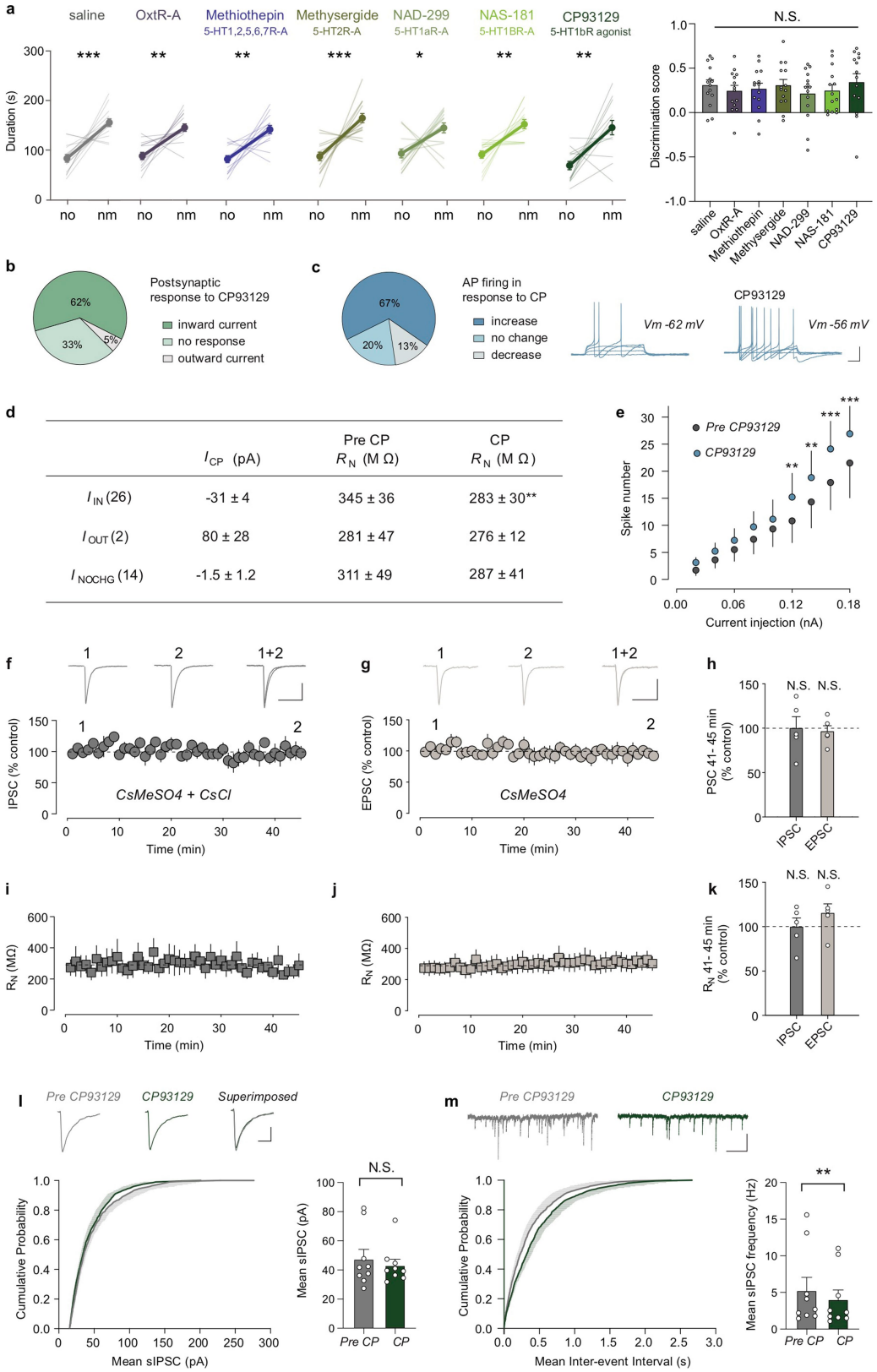

	I_{CP} (pA)	Pre CP R_N (M Ω)	CP R_N (M Ω)
I_{IN} (26)	-31 ± 4	345 ± 36	283 ± 30**
I_{OUT} (2)	80 ± 28	281 ± 47	276 ± 12
I_{NOCHG} (14)	-1.5 ± 1.2	311 ± 49	287 ± 41

Extended Data Fig. 8 | See next page for caption.

Extended Data Fig. 8 | Effects of CP93129 on dCA2-projecting MS neurons. **a**, Sociability is not affected by MS infusion of indicated drugs. Duration in chamber with no or nm (left) and discrimination scores (right) ($F_{5,78} = 0.3144$, $P = 0.9029$; $n = 14$). **b**, Pie chart summarizing postsynaptic responses of EGFP-positive cells in CP93129 (2 or 5 µM, $n = 42$). **c**, Pie chart illustrating action potential (AP) firing changes in CP93129 (left, $n = 15$). Representative traces -/+ CP93129 (right). Vm refers to unclamped resting membrane potential. Scale bars, 25 mV, 100 ms. **d**, Effects of CP93129 on MS neurons projecting to dCA2. Number of cells per current are indicated in parentheses ($t_{25} = 3.461$, $P = 0.002$; $n = 26$) (NOCHG, no change). **e**, Quantification of action potential firing as function of current injection for dCA2-projecting MS neurons with increased firing in CP93129 ($P = 0.001$; $n = 10$). **f**, Summary time course of IPSC responses in D-AP5 and NBQX with a pipette solution comprising CsMeSO4+CsCl. Representative traces above shown at indicated time points. Scale bars, 100 pA, 50 ms, $n = 5/2$. **g**, Summary time course of EPSC responses in picrotoxin while recording with a pipette solution comprising CsMeSO4. Representative traces above shown at indicated time points. Scale bars, 50 pA, 10 ms, $n = 5/3$. **h**, Amplitudes of IPSCs ($t_4 = 0.0285$, $P = 0.979$, $n = 5$) and EPSCs ($t_4 = 0.593$, $P = 0.585$, $n = 5$) averaged over the last 5 min of recording as a percentage of the first 3 min of baseline recording. **i**, **j**, Corresponding input resistance measurements for cells shown in **f** and **g**. **k**, R_N of IPSC ($t_4 = 0.058$, $P = 0.957$, $n = 5$) and EPSC ($t_4 = -1.409$, $P = 0.232$, $n = 5$) recordings averaged over the last 5 min of recording as a percentage of the first 3 min of baseline recording. **l**, Recordings of spontaneous inhibitory postsynaptic currents (sIPSCs) from EGFP-positive cells before and after bath-application of CP93129 (CP). Cumulative probability plot of sIPSC amplitudes with representative traces (above, scale bars, 15 pA, 15 ms, $n = 9/6$ (cells/mice)). Bar graph shows effect of CP93129 on mean IPSC amplitude. **m**, Cumulative probability plot of sIPSC inter-event intervals with representative traces (above, scale bars, 50 pA, 0.5 s, $n = 9/6$). Bar graph shows effect of CP93129 on mean IPSC frequency. Statistical tests: **a**, duration: two-tailed paired Student's *t*-test; discrimination scores: one-way ANOVA with Tukey's post-hoc test. **d**, **h**, **k**, Two-tailed paired Student's *t*-test. **e**, Repeated measures two-way ANOVA with Sidak's multiple comparison post-hoc test. **l**, **m**, tTwo-tailed Wilcoxon signed rank test. N.S. = not significant, $^*P < 0.05$, $^{**}P < 0.01$, $^{***}P < 0.001$. Error bars and shading denote s.e.m.

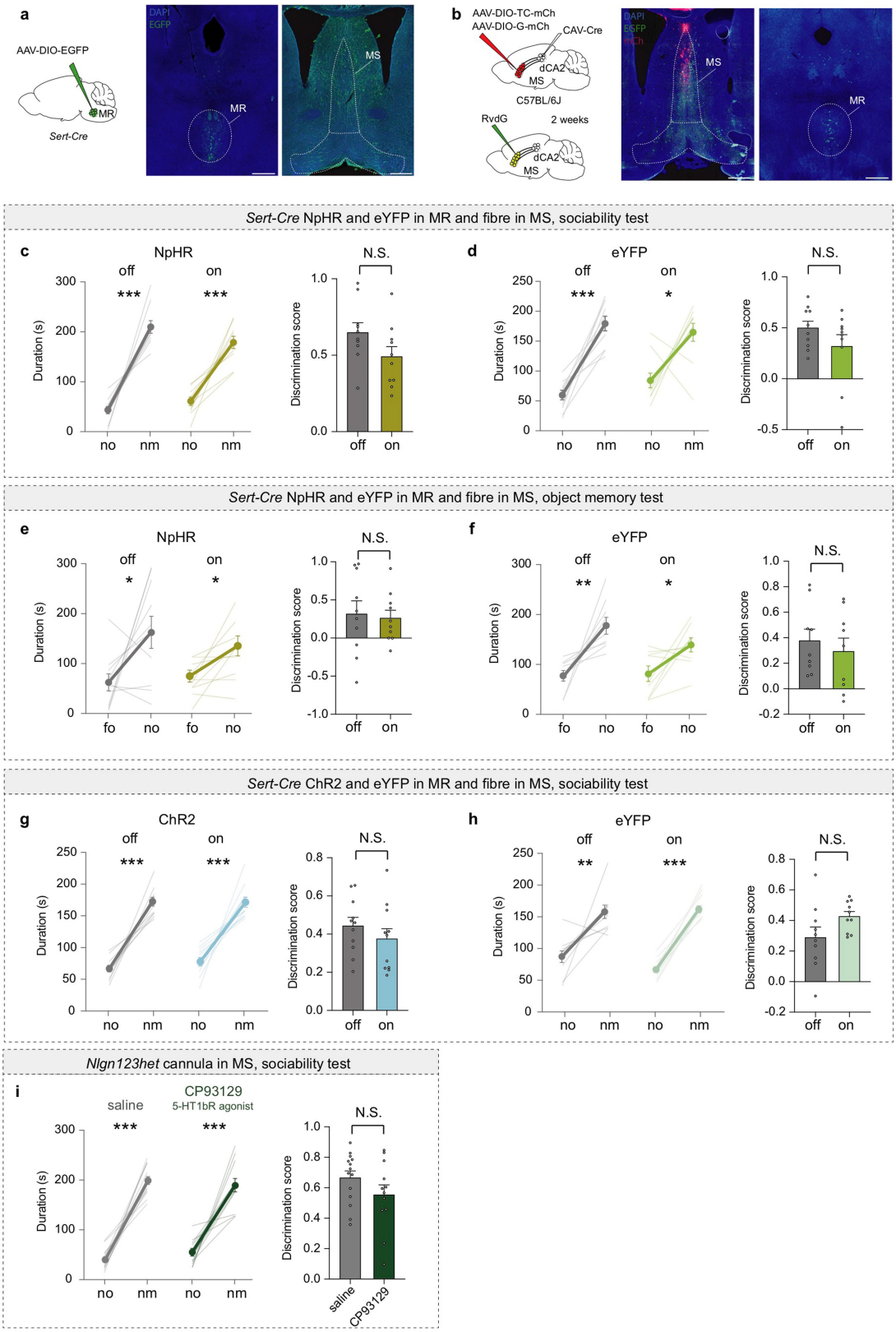

Extended Data Fig. 9 | See next page for caption.

Extended Data Fig. 9 | Optogenetic inhibition or excitation of 5-HT inputs in the MS does not alter sociability and object memory. a, Schematic of virus injection (left) and representative images of the injection site in the median raphe (MR) on the left and the EGFP-positive axons in the MS (right). $n = 5$. **b**, Schematic of virus injections to perform TRIO (left) and representative images of the injection site in the MS and the GFP-positive cells in the MR (right). $n = 3$. Scale bars = 500 µm. **c**, **d**, Duration in chamber with no or nm (left) and discrimination scores (right) (**c**: $t_9 = 1.834$; $P = 0.0998$; $n = 10$. **d**: $P = 0.3750$; $n = 10$). **e**, **f**, Duration in chamber with fo or no (left) and discrimination scores (right) (**e**: $t_9 = 0.2418$, $P = 0.8143$; $n = 10$. **f**: $t_8 = 0.6029$, $P = 0.5632$, $n = 9$). **g**, **h**, Duration in chamber with no or nm (left) and discrimination scores (right) (**g**: $t_{10} = 0.9294$, $P = 0.3746$; $n = 11$. **h**: $t_9 = 1.518$, $P = 0.1633$; $n = 10$). **i**, Duration in chamber with no or nm (left) and discrimination scores (right) ($t_{11} = 1.52$, $P = 0.152$; saline: $n = 12$, CP93129: $n = 14$). Statistical tests: **d**, eYFP on duration and discrimination score: two-tailed Wilcoxon signed rank test. All other data in this figure were analysed by two-tailed paired Student's *t*-test. N.S. = not significant, $^*P < 0.05$, $^{**}P < 0.01$, $^{***}P < 0.001$. Error bars denote s.e.m.

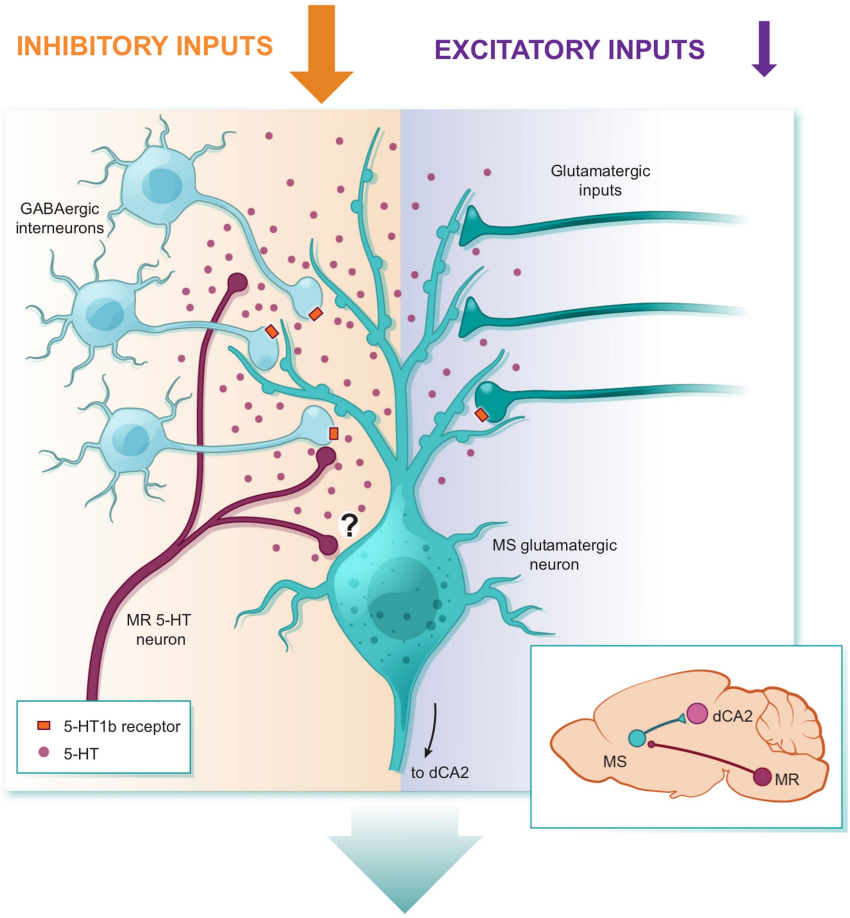

Extended Data Fig. 10 | Model illustrating 5-HT action on dCA2-projecting MS neurons. During a novel social encounter, 5-HT diffuses away from its release sites to bind to 5-HT_{1B}Rs on the terminals of MS GABAergic interneurons thereby inhibiting GABA release onto the dCA2-projecting glutamatergic MS neurons. 5-HT also can bind to 5-HT_{1B}Rs on presynaptic glutamatergic terminals to inhibit glutamate release but a smaller proportion of glutamatergic inputs express 5-HT_{1B}Rs. The net effect of 5-HT is to reduce local inhibition of dCA2-projecting MS neurons to a greater extent than its reduction of excitatory drive, thereby resulting in increased activity in these neurons. The question mark indicates that there may also be a direct effect of 5-HT on dCA2-projecting MS neurons. The inset on the right depicts the circuitry investigated in this study from the median raphe (MR) to the medial septum (MS) to dorsal CA2 (dCA2).

nature portfolio

Corresponding author(s): Robert Malenka

Last updated by author(s): Aug 4, 2021

Reporting Summary

Nature Portfolio wishes to improve the reproducibility of the work that we publish. This form provides structure for consistency and transparency in reporting. For further information on Nature Portfolio policies, see our Editorial Policies and the Editorial Policy Checklist.

Statistics

For all statistical analyses, confirm that the following items are present in the figure legend, table legend, main text, or Methods section.

n/a	Confirmed	
☐	☒	The exact sample size (*n*) for each experimental group/condition, given as a discrete number and unit of measurement
☐	☒	A statement on whether measurements were taken from distinct samples or whether the same sample was measured repeatedly
☐	☒	The statistical test(s) used AND whether they are one- or two-sided *Only common tests should be described solely by name; describe more complex techniques in the Methods section.*
☐	☒	A description of all covariates tested
☐	☒	A description of any assumptions or corrections, such as tests of normality and adjustment for multiple comparisons
☐	☒	A full description of the statistical parameters including central tendency (e.g. means) or other basic estimates (e.g. regression coefficient) AND variation (e.g. standard deviation) or associated estimates of uncertainty (e.g. confidence intervals)
☐	☒	For null hypothesis testing, the test statistic (e.g. *F*, *t*, *r*) with confidence intervals, effect sizes, degrees of freedom and *P* value noted *Give P values as exact values whenever suitable.*
☒	☐	For Bayesian analysis, information on the choice of priors and Markov chain Monte Carlo settings
☒	☐	For hierarchical and complex designs, identification of the appropriate level for tests and full reporting of outcomes
☐	☒	Estimates of effect sizes (e.g. Cohen's *d*, Pearson's *r*), indicating how they were calculated

Our web collection on statistics for biologists contains articles on many of the points above.

Software and code

Policy information about availability of computer code

Data collection	Axograph X 1.7.6, Igor Pro 6.37 (Wavemetrics), Minianalysis 6.0.7 (Synaptosoft) were used for the acquisition of electrophysiological recordings. Fibre photometry data was acquired via the Synapse software (Tucker-Davies Technologies).
Data analysis	Behavioral experiments were analysed using the video tracking system (BIOBSERVE, Version 3.01). Axograph X 1.7.6, Igor Pro 6.37 (Wavemetrics), Minianalysis 6.0.7 (Synaptosoft) were also used for the analysis of electrophysiological recordings. MATLAB_R2019b (Mathworks, Inc) was used for analysis of fibre photometry data.

For manuscripts utilizing custom algorithms or software that are central to the research but not yet described in published literature, software must be made available to editors and reviewers. We strongly encourage code deposition in a community repository (e.g. GitHub). See the Nature Portfolio guidelines for submitting code & software for further information.

Data

Policy information about availability of data

All manuscripts must include a data availability statement. This statement should provide the following information, where applicable:

- Accession codes, unique identifiers, or web links for publicly available datasets
- A description of any restrictions on data availability
- For clinical datasets or third party data, please ensure that the statement adheres to our policy

The datasets generated and analysed during this study are included in this published article and its supplementary information files. Any additional data generated and/or analysed during this study are available from the corresponding author upon reasonable request.

Field-specific reporting

Please select the one below that is the best fit for your research. If you are not sure, read the appropriate sections before making your selection.

☒ Life sciences ☐ Behavioural & social sciences ☐ Ecological, evolutionary & environmental sciences

For a reference copy of the document with all sections, see nature.com/documents/nr-reporting-summary-flat.pdf

Life sciences study design

All studies must disclose on these points even when the disclosure is negative.

Sample size	No statistical methods were used to predetermine sample sizes, which were based on work in previous publications (ref. 8: Walsh, et al. 2018; Dolen, et al. 2013, Nature, 501(7466):179-84). Sample sizes of 6–15 animals were sufficient to determine significance both in behaviour tests and electrophysiological recordings.
Data exclusions	Out of the >300 animals used in our experiments, <5% were excluded based of the lack of transgene expression in the targeted brain region.
Replication	All attempts at replication were successful. Reported findings were reproduced across animals in anatomical, imaging and behavioural experiments as well as across cells/ animals in physiology experiments. The total number of animals and cells is reported for all experiments. For representative images shown in the main figures, number of replicates is described in the Statistics and Reproducibility section of the methods. The number of replicates for representative images is listed directly in the Extended data figures.
Randomization	Animals were randomized by cage prior to surgeries. For example, if there were 30 mice in an experiment, with five mice per cage, mice were randomly assigned to be in eYFP or ChR2 groups in a counterbalanced fashion.
Blinding	All experiments were conducted in a blind manner such that assays were conducted and analyzed without knowledge of the specific manipulation being performed.

Reporting for specific materials, systems and methods

We require information from authors about some types of materials, experimental systems and methods used in many studies. Here, indicate whether each material, system or method listed is relevant to your study. If you are not sure if a list item applies to your research, read the appropriate section before selecting a response.

Materials & experimental systems

n/a	Involved in the study
☐	☒ Antibodies
☐	☐ Eukaryotic cell lines
☐	☐ Palaeontology and archaeology
☐	☒ Animals and other organisms
☐	☐ Human research participants
☐	☐ Clinical data
☐	☐ Dual use research of concern

Methods

n/a	Involved in the study
☐	☐ ChIP-seq
☐	☐ Flow cytometry
☐	☐ MRI-based neuroimaging

Antibodies

Antibodies used	Primary antibodies: rabbit polyclonal anti-CaMKII 1:200 (Thermo Fisher Scientific, PA5-38239), rabbit polyclonal anti-choline acetyltransferase (ChAT) 1:200 (Millipore Sigma, AB143), chicken anti-GFP 1:1000 (Aves labs, GFP-1020). Secondary antibodies: goat anti-rabbit Alexa Fluor 546 1:500 (Thermo Fisher Scientific, A11035), donkey anti-chicken Alexa Fluor 488 (Jackson Immuno Research Labs, 703545155).
Validation	IHC results were compared with published data for known distribution of labelled structures. anti-CaMKII: Xu et al., 2019, J. Neurosc., 39(7):1222–1235 anti-ChAT: Machold et al., 2005, Neuron, 48(1):17-24 anti-GFP: Beier et al., 2017, Nature, 549(7672):345-350

Eukaryotic cell lines

Policy information about cell lines

Cell line source(s)	
Authentication	

Mycoplasma contamination	
Commonly misidentified lines (See ICLAC register)	

Palaeontology and Archaeology

Specimen provenance	*Provide provenance information for specimens and describe permits that were obtained for the work (including the name of the issuing authority, the date of issue, and any identifying information). Permits should encompass collection and, where applicable, export.*
Specimen deposition	*Indicate where the specimens have been deposited to permit free access by other researchers.*
Dating methods	*If new dates are provided, describe how they were obtained (e.g. collection, storage, sample pretreatment and measurement), where they were obtained (i.e. lab name), the calibration program and the protocol for quality assurance OR state that no new dates are provided.*

☐ Tick this box to confirm that the raw and calibrated dates are available in the paper or in Supplementary Information.

Ethics oversight	*Identify the organization(s) that approved or provided guidance on the study protocol, OR state that no ethical approval or guidance was required and explain why not.*

Note that full information on the approval of the study protocol must also be provided in the manuscript.

Animals and other organisms

Policy information about studies involving animals; ARRIVE guidelines recommended for reporting animal research

Laboratory animals	Female and male C57BL/6J (JAX, 664), TRAP2, TRAP2;Ai14 (gift of L. Luo), B6.Cg-Tg(Amigo2-cre)1Sieg/J (Amigo2-Cre, JAX, 30315), Tg(Slc6a4-cre)ET33Gsat (Sert-Cre, JAX, 3836639) and Nlgn123 het mice were used as experimental subjects. Strictly transgene-carrying male mice were crossed with wild-type female C57BL/6J mice sourced commercially to produce heterozygous offspring. Nlgn123het mice were generated by breeding Nlgn123cKO male mice (gift of T.C. Sudhof) with B6.C-Tg(CMV-cre)1Cgn/J (JAX, 6054) females. Mice were weaned at 21 days old and housed with 2-5 mice per cage. Behavioural experiments were performed when mice were 7-14 weeks old. All mice were housed at a temperature of approximately 20°C and ~55% humidity, on a 12-hour light/dark cycle with food and water ad libitum and behavioural experiments were conducted during the same circadian period (7:00-19:00).
Wild animals	No wild animals were used.
Field-collected samples	No samples were field-collected.
Ethics oversight	All procedures complied with the animal care standards set forth by the National Institutes of Health and were approved by the Stanford University Administrative Panel on Laboratory Animal Care and Administrative Panel of Biosafety.

Note that full information on the approval of the study protocol must also be provided in the manuscript.

Human research participants

Policy information about studies involving human research participants

Population characteristics	*Describe the covariate-relevant population characteristics of the human research participants (e.g. age, gender, genotypic information, past and current diagnosis and treatment categories). If you filled out the behavioural & social sciences study design questions and have nothing to add here, write "See above."*
Recruitment	*Describe how participants were recruited. Outline any potential self-selection bias or other biases that may be present and how these are likely to impact results.*
Ethics oversight	*Identify the organization(s) that approved the study protocol.*

Note that full information on the approval of the study protocol must also be provided in the manuscript.

Clinical data

Policy information about clinical studies

All manuscripts should comply with the ICMJE guidelines for publication of clinical research and a completed CONSORT checklist must be included with all submissions.

Clinical trial registration	*Provide the trial registration number from ClinicalTrials.gov or an equivalent agency.*
Study protocol	*Note where the full trial protocol can be accessed OR if not available, explain why.*
Data collection	*Describe the settings and locales of data collection, noting the time periods of recruitment and data collection.*
Outcomes	*Describe how you pre-defined primary and secondary outcome measures and how you assessed these measures.*

Dual use research of concern

Policy information about dual use research of concern

Hazards

Could the accidental, deliberate or reckless misuse of agents or technologies generated in the work, or the application of information presented in the manuscript, pose a threat to:

No	Yes	
☒	☐	Public health
☒	☐	National security
☒	☐	Crops and/or livestock
☒	☐	Ecosystems
☒	☐	Any other significant area

Experiments of concern

Does the work involve any of these experiments of concern:

No	Yes	
☒	☐	Demonstrate how to render a vaccine ineffective
☒	☐	Confer resistance to therapeutically useful antibiotics or antiviral agents
☒	☐	Enhance the virulence of a pathogen or render a nonpathogen virulent
☒	☐	Increase transmissibility of a pathogen
☒	☐	Alter the host range of a pathogen
☒	☐	Enable evasion of diagnostic/detection modalities
☒	☐	Enable the weaponization of a biological agent or toxin
☒	☐	Any other potentially harmful combination of experiments and agents

ChIP-seq

Data deposition

☐ Confirm that both raw and final processed data have been deposited in a public database such as GEO.

☐ Confirm that you have deposited or provided access to graph files (e.g. BED files) for the called peaks.

Data access links *May remain private before publication.*	*For "Initial submission" or "Revised version" documents, provide reviewer access links. For your "Final submission" document, provide a link to the deposited data.*
Files in database submission	*Provide a list of all files available in the database submission.*
Genome browser session (e.g. UCSC)	*Provide a link to an anonymized genome browser session for "Initial submission" and "Revised version" documents only, to enable peer review. Write "no longer applicable" for "Final submission" documents.*

Methodology

Replicates	*Describe the experimental replicates, specifying number, type and replicate agreement.*
Sequencing depth	*Describe the sequencing depth for each experiment, providing the total number of reads, uniquely mapped reads, length of reads and whether they were paired- or single-end.*
Antibodies	*Describe the antibodies used for the ChIP-seq experiments; as applicable, provide supplier name, catalog number, clone name, and lot number.*
Peak calling parameters	*Specify the command line program and parameters used for read mapping and peak calling, including the ChIP, control and index files used.*
Data quality	*Describe the methods used to ensure data quality in full detail, including how many peaks are at FDR 5% and above 5-fold enrichment.*
Software	*Describe the software used to collect and analyze the ChIP-seq data. For custom code that has been deposited into a community repository, provide accession details.*

Flow Cytometry

Plots

Confirm that:

☐ The axis labels state the marker and fluorochrome used (e.g. CD4-FITC).

☐ The axis scales are clearly visible. Include numbers along axes only for bottom left plot of group (a 'group' is an analysis of identical markers).

☐ All plots are contour plots with outliers or pseudocolor plots.

☐ A numerical value for number of cells or percentage (with statistics) is provided.

Methodology

Sample preparation	*Describe the sample preparation, detailing the biological source of the cells and any tissue processing steps used.*
Instrument	*Identify the instrument used for data collection, specifying make and model number.*
Software	*Describe the software used to collect and analyze the flow cytometry data. For custom code that has been deposited into a community repository, provide accession details.*
Cell population abundance	*Describe the abundance of the relevant cell populations within post-sort fractions, providing details on the purity of the samples and how it was determined.*
Gating strategy	*Describe the gating strategy used for all relevant experiments, specifying the preliminary FSC/SSC gates of the starting cell population, indicating where boundaries between "positive" and "negative" staining cell populations are defined.*

☐ Tick this box to confirm that a figure exemplifying the gating strategy is provided in the Supplementary Information.

Magnetic resonance imaging

Experimental design

Design type	*Indicate task or resting state; event-related or block design.*
Design specifications	*Specify the number of blocks, trials or experimental units per session and/or subject, and specify the length of each trial or block (if trials are blocked) and interval between trials.*
Behavioral performance measures	*State number and/or type of variables recorded (e.g. correct button press, response time) and what statistics were used to establish that the subjects were performing the task as expected (e.g. mean, range, and/or standard deviation across subjects).*

Acquisition

Imaging type(s)	*Specify: functional, structural, diffusion, perfusion.*
Field strength	*Specify in Tesla*
Sequence & imaging parameters	*Specify the pulse sequence type (gradient echo, spin echo, etc.), imaging type (EPI, spiral, etc.), field of view, matrix size, slice thickness, orientation and TE/TR/flip angle.*
Area of acquisition	*State whether a whole brain scan was used OR define the area of acquisition, describing how the region was determined.*

Diffusion MRI ☐ Used ☐ Not used

Preprocessing

Preprocessing software	*Provide detail on software version and revision number and on specific parameters (model/functions, brain extraction, segmentation, smoothing kernel size, etc.).*
Normalization	*If data were normalized/standardized, describe the approach(es): specify linear or non-linear and define image types used for transformation OR indicate that data were not normalized and explain rationale for lack of normalization.*
Normalization template	*Describe the template used for normalization/transformation, specifying subject space or group standardized space (e.g. original Talairach, MNI305, ICBM152) OR indicate that the data were not normalized.*
Noise and artifact removal	*Describe your procedure(s) for artifact and structured noise removal, specifying motion parameters, tissue signals and physiological signals (heart rate, respiration).*

Volume censoring | *Define your software and/or method and criteria for volume censoring, and state the extent of such censoring.*

Statistical modeling & inference

Model type and settings | *Specify type (mass univariate, multivariate, RSA, predictive, etc.) and describe essential details of the model at the first and second levels (e.g. fixed, random or mixed effects; drift or auto-correlation).*

Effect(s) tested | *Define precise effect in terms of the task or stimulus conditions instead of psychological concepts and indicate whether ANOVA or factorial designs were used.*

Specify type of analysis: ☐ Whole brain ☐ ROI-based ☐ Both

Statistic type for inference (See Eklund et al. 2016) | *Specify voxel-wise or cluster-wise and report all relevant parameters for cluster-wise methods.*

Correction | *Describe the type of correction and how it is obtained for multiple comparisons (e.g. FWE, FDR, permutation or Monte Carlo).*

Models & analysis

n/a	Involved in the study
☒	☐ Functional and/or effective connectivity
☒	☐ Graph analysis
☒	☐ Multivariate modeling or predictive analysis